# PERFORMANCE ANALYSIS OF DIVERSITY TECHNIQUES FOR OFDM AND BASE STATION COOPERATION

A THESIS

SUBMITTED TO THE DEPARTMENT OF ELECTRICAL AND ELECTRONICS ENGINEERING

AND THE INSTITUTE OF ENGINEERING AND SCIENCES

OF BILKENT UNIVERSITY

IN PARTIAL FULFILLMENT OF THE REQUIREMENTS

FOR THE DEGREE OF

MASTER OF SCIENCE

By

Hande Üzeler

January 2010

I certify that I have read this thesis and that in my opinion it is fully adequate, in scope and in quality, as a thesis for the degree of Master of Science.

Assist. Prof. Dr. Defne Aktaş (Supervisor)

I certify that I have read this thesis and that in my opinion it is fully adequate, in scope and in quality, as a thesis for the degree of Master of Science.

Prof. Dr. Erdal Arıkan

I certify that I have read this thesis and that in my opinion it is fully adequate, in scope and in quality, as a thesis for the degree of Master of Science.

Assoc. Prof. Dr. Ali Özgür Yılmaz

Approved for the Institute of Engineering and Sciences:

Prof. Dr. Mehmet Baray
Director of Institute of Engineering and Sciences

# ABSTRACT

## PERFORMANCE ANALYSIS OF DIVERSITY TECHNIQUES FOR OFDM AND BASE STATION COOPERATION

Hande Üzeler
M.S. in Electrical and Electronics Engineering
Supervisor: Assist. Prof. Dr. Defne Aktaş
January 2010

The main goal of the next generation wireless communication systems is to provide high data rate services. In order to deal with performance-limiting challenges that include frequency selective fading channels, power and bandwidth constraints, multiple input multiple output (MIMO) and orthogonal frequency division multiplexing (OFDM) techniques have been proposed as effective techniques to combat fading and to provide high rate reliable transmission. In this thesis we first give an overview of WiMAX as an example of an OFDM system and study the performance of the WiMAX physical layer under different MIMO techniques. We also analyze space-frequency coding and propose a threaded algebraic space-time (TAST) based code.

Secondly, since the mobile bandwidth is an expensive and scarce resource, it seems likely that a high frequency reuse will be employed in the future cellular networks to increase spectral efficiency. This means that base stations (BSs) will operate in the same frequency band and therefore cause cochannel interference (CCI) to the users at other cells. CCI is an important performance degrading factor. Therefore our second aim is to investigate BS cooperation techniques to mitigate CCI. We assume that channel state information (CSI) is available at the cooperating BSs and analyze the performance gains due to cooperation when used in conjunction with Alamouti space-time coding.

*Keywords:* Multiple Input Multiple Output (MIMO), Orthogonal Frequency Division Multiplexing (OFDM), Space-Time Coding, Space-Frequency Coding, Base Station Cooperation, Distributed Space-Time Coding.

# ÖZET

## ÇEŞİTLEME TEKNİKLERİNİN DİKGEN FREKANS BÖLMELİ ÇOĞULLAMALI SİSTEMLERDE VE TELSİZ ERİŞİM TERMİNALLERİNİN İŞBİRLİĞİ ALTINDA BAŞARIMLARININ ANALİZİ

Hande Üzeler
Elektrik ve Elektronik Mühendisliği Yüksek Lisans
Tez Yöneticisi: Yar. Doç. Dr. Defne Aktaş
Ocak 2010

Yeni kuşak iletişim sistemlerinin ana amacı yüksek veri hızı sağlayabilmektir. Frekansa bağımlı sönümleme, bant genişliği ve güç kısıtlamaları gibi başarımı kısıtlayan etkenlerle mücadele etmek için çok girdili çok çıktılı (MIMO) ve dikgen frekans bölmeli çoğullama (OFDM) teknikleri sağladıkları güvenilir iletim ve frekans seçiciliğine karşı etkinliklerinden dolayı önerilmektedir. Bu tezde ilk önce OFDM tekniği için örnek olarak WiMAX (IEEE 802.16 standardı) tanıtıldıktan sonra fiziksel katmanın başarımı farklı MIMO teknikleri altında incelendi. Ayrıca cebirsel uzay-zaman kodlarını kullanarak bir uzay-frekans kodu önerildi.

Frekans spektrumu pahalı ve kıt bir kaynak olduğundan, gelecekteki hücresel ağların spektral verimliliği arttırmak için yüksek bir frekans yeniden kullanım faktörüne ihtiyaçları vardır. Bunun için telsiz erişim terminallerinin aynı frekans bantını kullanması gerekmektedir ve bu durum kullanıcıların önemli ölçüde ortak kanal girişimine (CCI) maruz kalmalarına neden olmaktadır. Ortak kanal girişimi başarımı kısıtlayan önemli bir etmendir bu yüzden tezin ikinci amacı ortak kanal girişimini azaltan telsiz erişim terminalleri işbirliği tekniklerini incelemektir. Kanal durum bilgisinin telsiz erişim terminallerinde mevcut olduğu varsayılarak telsiz erişim terminalleri işbirliği tekniklerinin Alamouti uzay-zaman kodlaması ile birlikte kullanıldığında oluşan başarım kazançları analiz edildi.

*Anahtar Kelimeler:* Çok Girdili Çok Çıktılı Sistemler, Dikgen Frekans Bölmeli Çoğullama, Uzay-Zaman Kodlama, Uzay-Frekans Kodlama, Telsiz Erişim Terminallerinin İşbirliği, Dağıtılmış Uzay-Zaman Kodlama

# ACKNOWLEDGMENTS

I would like to express my sincere gratitude to my supervisor Assist. Prof. Dr. Defne Aktaş for her guidance, support, and encouragement throughout the course of this work. I am also grateful to Professors Erdal Arıkan and Ali Özgür Yılmaz for being members of my thesis defense committee.

I would also like to thank TUBITAK Career Program 107E199 Project and European Commission $7^{th}$ Framework Programme WiMAGIC Project for their financial support.

Finally, the writing of this thesis would not have been possible without the continual support of my family and friends, to whom I am indebted.

# Contents

# List of Figures

# List of Tables

# List of Abbreviations

| | |
|---|---|
| AMC | Adaptive Modulation and Coding |
| BER | Bit Error Rate |
| BLER | Block Error Rate |
| BS | Base Station |
| CCI | Cochannel Interference |
| CC | Convolutional Coding |
| CSI | Channel State Information |
| CTC | Convolutional Turbo Coding |
| CP | Cyclic Prefix |
| FEC | Forward Error Correction |
| FFT | Fast Fourier Transform |
| i.i.d. | Independent and Identically Distributed |
| ICI | Intercarrier Interference |
| ISI | Intersymbol Interference |
| MS | Mobile Station |
| MIMO | Multiple Input Multiple Output |
| ML | Maximum Likelihood |
| NLOS | Non-Line-of-Sight |
| OFDM | Orthogonal Frequency Division Multiplexing |
| OFDMA | Orthogonal Frequency Division Multiple Access |
| pcu | Per Channel Use |
| PEP | Pairwise Error Probability |
| PUSC | Partial Usage of Subcarriers |
| PHY Layer | Physical Layer |
| SINR | Signal to Interference plus Noise Ratio |
| SLNR | Signal to Leakage plus Noise Ratio |
| SF | Space-Frequency |
| ST | Space-Time |
| STC | Space-Time Code |
| SM | Spatial Multiplexing |
| SNR | Signal to Noise Ratio |
| SVD | Singular Value Decomposition |
| TAST | Threaded Algebraic Space-Time |
| WiMAX | Worldwide Interoperability for Microwave Access |
| ZF | Zero-Forcing |

**Dedicated to my family ...**

# Chapter 1

# Introduction

In recent years, there has been a rapid growth in wireless communications driven by growing demand for emerging wideband services such as high-speed Internet access and high-quality multimedia transmission. The frequency spectrum or bandwidth is a limited resource, therefore to meet the demand for high data rate services the design of wireless communication systems that are capable of providing increased data rates and improved performance have become an active area of research.

The wireless channel presents a challenge for reliable communications because of factors such as multipath, mobility of the user or the surrounding environment and delays associated with multipath. Multipath occurs because a transmitted signal can be reflected, diffracted and refracted by the objects in the environment before reaching the receiver. Furthermore, the signal may follow multiple paths between the transmit and the receive antenna such that the received signal will consist of multiple delayed and attenuated copies of the transmitted signal which may add up destructively. The combination of all of these factors is called fading, a phenomenon which decreases the signal to noise ratio (SNR) of the received signal leading to a performance loss [1].

## 1.1 Motivation

One of the most promising solutions for combating fading and to improve system performance is to use multiple antennas at the transmitter and receiver. In a multiple-input multiple-output (MIMO) system with $M_T$ transmit and $M_R$

receive antennas, diversity can be obtained from the $M_T \times M_R$ links between the transmitter and receiver. The basic idea behind diversity is to provide to the receiver a number of different replicas of the same transmitted signal such that these replicas may be combined in some way to improve the overall performance.

However, when MIMO broadband channels are used for high data rate communication, multipath causes the channel to become a frequency selective channel which results in intersymbol interference (ISI) at the receiver and degrades the performance. In this case orthogonal frequency division multiplexing (OFDM), which is a multicarrier modulation scheme, may be used because it has high spectral efficiency and robustness against frequency selective channels. In OFDM, a frequency selective channel is transformed into a number of parallel frequency-flat subchannels, thereby reducing the receiver complexity by eliminating the need for time-domain equalization. The combination of OFDM and MIMO is a promising technique to meet the increasing high speed and reliability demands of the future. In fact, MIMO-OFDM is implemented in the IEEE 802.16 (Worldwide Interoperability for Microwave Access (WiMAX)) standard.

The first objective of this thesis is to implement and simulate the MIMO techniques proposed in the IEEE 802.16 physical (PHY) layer using Matlab in order to have a better understanding of the standard and the system performance. This involves studying, through simulations, the various PHY layer coding schemes and MIMO techniques in the form of bit error rate (BER) and block error rate (BLER) performance under realistic channel models. As a part of the WiMAGIC project, which is an industry-driven research project aiming to develop novel and innovative solutions for WiMAX, our main goal is to investigate the existing MIMO techniques and make contributions towards new MIMO techniques which may be proposed to be employed in next generation WiMAX systems (IEEE 802.16m).

The second objective is to analyze the achievable gains when multiple base stations (BSs) cooperate with each other in an OFDM system. Most of the existing work on BS cooperation schemes consider single carrier systems therefore it is of interest to evaluate the performance of such schemes under an OFDM scenario since OFDM based systems, such as WiMAX, are expected to be in wide use in the future.

## 1.2 Literature Survey

Information theoretic results show that the capacity of a single link MIMO system with $M_T$ transmit and $M_R$ receive antennas increases linearly with $\min(M_T, M_R)$ [2,3]. However, for single-input single-output (SISO) channels capacity increases logarithmically with SNR therefore, the capacity of MIMO can be $\min(M_T, M_R)$ times larger than the SISO capacity. Therefore a significant capacity increase can be achieved by MIMO systems without increasing the transmit power and expanding the bandwidth.

Several practical transmission schemes have been proposed that utilize the MIMO channel in different ways, e.g., spatial multiplexing or space-time coding. In spatial multiplexing different signals are transmitted simultaneously by the transmit antennas in the same frequency band to provide a capacity gain which increases with the number of antennas. The first high data rate architecture was the Bell-Labs layered space-time architecture (BLAST) proposed in [4] which achieved the theoretical capacity limits of the MIMO architecture. In BLAST, multiple parallel data streams are spatially multiplexed and transmitted simultaneously on the same frequency through all transmit antennas. With rich multipath propagation, these different streams are separated at the receiver based on their distinct spatial signatures. However, due to exponential complexity of the optimal receivers, for practical implementations suboptimal receiver structures are used resulting in performance loss. Furthermore, inherent diversity in the channel is not exploited to its fullest extent.

For reliable communications, high spectral efficiency must be accompanied with low error rate. MIMO systems offer significant diversity advantages by exploiting multiple antennas at both the transmitter and receiver in order to obtain transmit and receive diversity and therefore increase the reliability of the system. Space-time (ST) coding relies on simultaneously coding across space and time to achieve diversity gain without sacrificing bandwidth [5].

The performance criteria for ST codes were derived in [6] and the diversity and coding gain associated with ST codes were also defined. Diversity gain describes the asymptotic decrease of the error rate as a function of SNR and coding gain describes the vertical shift of the error curve.

Over the years many different ST codes were described which can be classified into two major classes: ST trellis codes (STTC) and ST block codes (STBC).

STTC employ complex trellis encoding across multiple transmit antennas. When the number of antennas is fixed, the decoding complexity of STTC (measured by the number of trellis states at the decoder) increases exponentially as a function of the diversity level and transmission rate [6].

To achieve linear processing at the receiver, in [7] Alamouti proposed a novel transmit STBC diversity scheme where the transmitted symbols are mapped to a 2x2 space-time orthogonal transmission matrix. The orthogonal design achieves maximum likelihood (ML) decoding with linear processing per transmitted symbol. Extending Alamouti's work, [8] proposed more general schemes referred to as orthogonal space-time block codes (OSTBC) for more than two transmit antennas. They showed that the orthogonal design couldn't provide full rate (not more than rate 3/4 symbols per channel use (pcu)) for more than two transmit antennas with complex constellations. STBC has a very simple decoding process while retaining the full diversity. The STBC scheme supports maximum likelihood (ML) detection based only on linear processing at the receiver. However, STBC can not provide an additional coding gain. Thus, STBC is typically concatenated with a bandwidth-efficient outer code.

To achieve spatial multiplexing gains with improved error performance some ST codes with rate greater than 1 symbol/pcu have been proposed [9, 10]. The increased spectral efficiency results in increased decoding complexity. Another class of ST codes based on algebraic number theory was proposed to achieve full diversity and high rate. In [11] threaded algebraic space-time (TAST) coding was proposed which made use of the layering concept. Here an algebraic code component [12, 13] is assigned to each thread and interleaved over space and time. A phase rotation is also applied to the layers such that the coded symbols can be sent as if they are transparent to each other. These codes also result in high decoder complexity due to joint detection of layers.

Most ST codes were developed for frequency nonselective (flat) channels and when used in broadband wireless communications, the frequency selective nature of the channel results in performance degradation due to ISI. OFDM is one of the most promising techniques for mitigating ISI without time domain equalization and it offers high spectral efficiency [14].

In frequency selective MIMO channels there is an additional source of diversity due to the multiple propagation paths between the transmit and receive antennas. This source of diversity is called frequency diversity and space-frequency (SF) coding has been proposed to combine the advantages of MIMO

and OFDM systems and exploit the spatial and frequency diversity available in the system [15–19]. In this coding scheme two-dimensional coding is applied to distribute symbols across space (transmit antennas) and frequency (OFDM subcarriers). The first SF coding scheme was proposed in [15] where existing ST codes were used by replacing the time domain with the frequency domain. In a straightforward way of realizing SF coding for two transmit antennas is to directly spread the Alamouti code over two subcarriers in one OFDM symbol [16].

The performance criteria for SF-coded MIMO-OFDM systems were derived in [18] and [20]. The maximum achievable diversity order was established as $M_T M_R L$, where $L$ is the number of delay paths. It was also shown that in general existing ST codes cannot exploit the frequency diversity available in the frequency selective MIMO channel and it was suggested that a new code design procedure will have to be developed for MIMO-OFDM systems. When ST codes were directly used as SF codes the potential multipath diversity offered by the frequency selective channel is not exploited.

In [21], the authors of [18] proposed a SF code construction method by multiplying the input symbols with a part of the discrete Fourier transform (DFT) matrix. The resulting SF codes achieve full diversity at the expense of bandwidth efficiency. In [19] a systematic design of full diversity SF block codes were proposed. This scheme relies on repeating each row of the underlying ST code matrix on $L$ different subchannels in the same OFDM symbol and therefore incurs spectral efficiency loss. The authors later proposed a design of full rate full diversity SF codes in [22]. In this scheme the information symbol vector is first coded via an algebraic rotation matrix and then mapped to different antennas and OFDM subcarriers. This way a rate of 1 symbol/pcu is achieved. It is important to choose the rotation matrix carefully such that signal space diversity can be obtained [23]. This idea was further developed in [24] by incorporating the TAST framework to increase spectral efficiency and some examples of code designs were given. Inspired by this, we will investigate the performance of TAST SF codes.

The idea of coding across multiple OFDM symbols resulting in space-time-frequency (STF) codes was proposed in [24, 25]. Full diversity is only achievable if the number of OFDM symbols over which data is encoded is not smaller than the number of independently fading OFDM symbols spanned over one STF codeword. Therefore with the assumption that the MIMO channel stays constant over multiple OFDM symbols, it was shown that STF codes could not achieve

any additional diversity compared to SF codes. STF codes incur longer decoding delay and higher decoding complexity.

The techniques mentioned above focus on single cell single-user MIMO systems. In cellular wireless systems BSs communicate with mobile stations (MSs) in their own cell. In conventional wireless systems, the co-existing BSs do not cooperate with each other. BSs transmit individually to their respective users and users treat the transmissions from other BSs as interference such that a mobile usually experiences several comparable and weak links from surrounding BSs. Therefore multiuser multicellular networks are limited by intercell cochannel interference (CC). This interference may be avoided by using frequency reuse at the expense of reduced spectral efficiency.

An alternative to the above noncooperative transmission scheme where each BS transmits to its respective MS is a cooperative transmission structure. It has been shown that performance gains are possible in multicell systems which use BS cooperation [26]. Since BSs are connected to each other via a high-speed optical fiber backbone, they can reliably exchange information among themselves. Therefore CC mitigation may be carried out at the transmitter (BS) side in the downlink, where complex structure and advanced processing can be more easily accommodated, if channel state information (CSI) can be obtained at the transmitter side either through uplink estimation or through a feedback channel. This may be possible for low user mobility scenarios such as indoor or outdoor pedestrian environments. Thus it is possible to coordinate the BS transmissions in order to mitigate CC in the downlink such that the MSs may receive useful signals, as opposed to interferences, from the cooperating BSs.

The information-theoretic characterization of the maximum sum capacity of MIMO broadcast systems with perfect CSI was based on the dirty-paper precoding technique [27]. It has been shown that the maximum sum capacity of a MIMO broadcast system with perfect CSI may be achieved by using dirty-paper codes [28]. However, due to the complexity of these schemes practical dirty-paper codes are not available. This has prompted the development of practical, suboptimal alternatives which can be categorized as linear transmission schemes such as zero-forcing (ZF) and minimum mean square error (MMSE) based precoding.

The ZF schemes aim to perfectly cancel out the CC observed at each user by determining transmit beamformer weights which will force the interference to zero. Recently a ZF beamforming scheme making use of the pseudo-inverse of the channel matrix has been considered in [29] for the multiple-input single-output

(MISO) downlink setup under sum power constraints. It was shown that a ZF beamforming strategy can achieve the same asymptotic sum rate as the optimal dirty paper coding scheme as the number of users goes to infinity. Some other important ZF schemes have been proposed in [30–32]. The ZF schemes require that the number of transmit antennas be larger than or equal to sum of receive antennas of all users. When this condition is not met user scheduling algorithms may be implemented to ensure the dimension requirements.

Many iterative algorithms have also been proposed. For example the scheme in [31] is further improved in [33] by finding the transmit-receive antenna weights iteratively. We will not consider iterative algorithms here due to complexity issues.

Some schemes aim to choose the transmit beamformers in order to maximize signal to interference plus noise ratio (SINR). In this case the choice of one users beamformer may affect the crosstalk experienced by other users. Hence, the SINR values of all users are coupled, which makes SINR-based downlink beamforming a complicated task. The solution can be obtained iteratively due to the coupled nature of the optimization problem.

The uplink downlink duality has been used for the beamforming problem to maximize SINR. In [34–36], the uplink-downlink duality concept is introduced to find the optimum transmit-receive antenna weights and to allocate downlink power. The authors first show that the downlink SINR can be designed to be equal to the maximum uplink SINR under the same total available power but with a different power allocation in the downlink and uplink. They then propose a method to find the transmit weights and transmission powers that maximize the individual downlink SINR by solving its dual uplink equivalence.

An alternative approach to designing transmit beamforming vectors is given in [37] based on the concept of signal leakage. The term leakage is used to define the interference caused by the signal of a user on the remaining users and is a measure of how much signal power leaks into the other users.The criterion of choosing transmit weights is then based on maximizing signal to leakage plus noise ratio (SLNR). The advantage of this system is that the optimization problem becomes decoupled and there exists a closed form solution. However, it does not completely eliminate CC and therefore users will experience some residual interference.

## 1.3 Contributions of This Thesis

The aim of this thesis is first to conduct a comprehensive performance evaluation and comparison of the ST/SF techniques in realistic MIMO-OFDM systems, in particular for a WiMAX system. We propose a SF scheme which has superior performance and resilience to high user speeds.

Secondly we aim to evaluate the performance gains of cooperative transmission schemes to demonstrate the anticipated improvement of BS cooperation on the system performance while keeping the receiver complexity low. We propose a simple ZF scheme which performs as well as the no CC case.

## 1.4 Thesis Organization

The rest of the thesis is organized as follows. In Chapter 2, we will introduce some basic principles and concepts of the MIMO system, including channel model and diversity techniques, and some space-time coding schemes which will be necessary in the next chapters.

In Chapter 3, OFDM systems and SF coding are discussed. Firstly an introduction to OFDM systems is given. Then the SF coding techniques are reviewed and an introduction to TAST framework is presented. The proposed TAST based SF code is explained in detail. The chapter is concluded with the simulation results of some ST and SF codes in a mobile WiMAX environment.

In Chapter 4, the cooperative transmission schemes are explained in detail and how transmitter beamformers are chosen such that CC is mitigated is discussed. We will compare these schemes in a multicell environment taking into account the large scale fading components which were previously ignored in the single-cell case. Furthermore, we will incorporate the Alamouti scheme into our cooperative model and will analyze its performance in multi-user multicell environment.

Finally, we summarize our conclusions and provide some research directions for the future in Chapter 6.

## 1.5 Notation

Upper case bold letters, $\mathbf{A}$, are used to denote matrices. Lower case bold letters, $\mathbf{a}$, are used to denote column vectors. $A_{ij}$ is the element of matrix $\mathbf{A}$ on $i$th row and $j^{th}$ column. $a_i$ denotes the $i^{th}$ element of column vector $\mathbf{a}$. E[.] is the statistical expectation operator. |.| indicates the absolute value. $(\cdot)^*$ represents the complex conjugation operation. $(\cdot)^T$, $(\cdot)^H$ and $(\cdot)^{-1}$ are the transpose, Hermitian transpose and inverse matrix operators respectively. $\mathbf{I}_N$ denotes the $N \times N$ identity matrix. The Kronecker product operator is denoted by $\otimes$.

# Chapter 2

# MIMO Communication Systems

Channel fading degrades the performance of wireless transmissions significantly, and becomes the bottleneck for increasing data rates. Diversity techniques are popularly used to reduce the effect of channel fading and improve the reliability of transmission without increasing the transmitted power and sacrificing bandwidth. In MIMO systems, space-time coding can achieve bandwidth-efficient spatial diversity provided by multiple antennas over the fading channel.

In this chapter, we will first describe the characteristics of wireless communication channels and give an introduction to MIMO systems. Then we will review diversity techniques and space-time coding schemes.

## 2.1 The Wireless Channel

Fading in a wireless channel can be classified into large and small-scale fading [1]. Large-scale fading describes the attenuation of the received signal over large distances and is caused by path loss which is a function of distance, and shadowing by large objects such as buildings and hills. We will consider large-scale fading in Chapter 4 because in multicellular environments path loss becomes an important factor. Path loss is modeled by the path loss exponent $n$ and the distance $d$ between the base station and user. We can express path loss associated with distance $d$ as $Pl = d^n$.

Small-scale fading refers to the dramatic changes of the received power level over small distances, or short periods of time. Small-scale fading is caused by the

constructive and destructive interference of the multiple signal paths between the transmitter and receiver. As a consequence of multipath fading, the deep fades experienced by the channel strongly impairs the performance of wireless communications. We can separate small-scale fading into two categories; fading effects due to delay spread and Doppler spread.

### 2.1.1 Fading Effects Due to Delay Spread

The received signal consists of the superposition of multiple copies of the transmitted signals that arrive at the receiver through different paths and at different times. This time dispersion is quantified by delay spread, denoted by $\sigma_\tau$. Depending on the relationship between delay spread and symbol period, $T_s$, fading is classified as either frequency-flat or frequency selective fading. Delay spread can be characterized by the coherence bandwidth, $B_c$, in the frequency domain. Coherence bandwidth defines the range of frequencies over which the channel may be considered as flat. Coherence bandwidth and delay spread are inversely proportional to each other.

The channel exhibits frequency flat fading when the symbol period is larger than the delay spread, i.e., $T_s >> \sigma_\tau$. In this case, all of the received multipath components of a symbol arrive within the symbol time duration, hence there is no channel-induced intersymbol interference (ISI) distortion. There is still performance degradation due to the destructive superposition of the individual multipath components which can yield a reduction in SNR. When there is loss in SNR due to flat fading, the appropriate mitigation technique is to improve the received SNR or use more robust transmission techniques, such as space-time codes which are discussed in Section 2.4.

The channel exhibits frequency selective fading when $T_s < \sigma_\tau$. In this case, the time duration over which the multipath components of a symbol arrive at the receiver exceeds the symbol duration and therefore cause ISI. Frequency selective channels can be modeled by a tapped delay line. For a fading channel with L different paths, the possibly time-variant impulse response can be expressed as

$$h(\tau;t) = \sum_{l=0}^{L-1} \alpha(l,t)\delta(\tau - \tau_l(t)), \tag{2.1}$$

where $\alpha(l,t)$ is the complex amplitude of the $l^{\text{th}}$ path and $\tau_l(t)$ is the time delay of the $l^{\text{th}}$ path at time $t$. In a non line-of-sight (NLOS) environment (i.e., when there

is no direct path between the transmitter and receiver), the impulse response $h(\tau;t)$ is modeled as a zero-mean complex Gaussian process and the envelope $|h(\tau;t)|$ has a Rayleigh distribution for any time $t$. Furthermore, the $\alpha(l,t)$'s are zero-mean, independent and identically distributed (i.i.d) complex Gaussian random variables.

We assume that $h(\tau;t)$ is wide-sense stationary and the autocorrelation function is defined as [38]

$$\phi_h(\tau_1,\tau_2;\Delta t) = E\left[h^*(\tau_1;t)h(\tau_2;t+\Delta t)\right] = \phi_h(\tau_1;\Delta t)\delta(\tau_1-\tau_2), \tag{2.2}$$

where $\Delta t$ is the observation time difference and the second equality follows from the fact that $\alpha(l,t)$'s are uncorrelated. If we let $\Delta t = 0$, the autocorrelation function $\phi_h(\tau_1;0) = \phi_h(\tau_1)$ is the average power output of the channel. For a path delay $\tau$, $\phi_h(\tau)$ is called the power delay profile of the frequency selective fading channel.

### 2.1.2 Fading Effects Due to Doppler Spread

The channel may also be time variable as a consequence of relative motion between transmitter and receiver, or because of mobility in the environment. The characterization of the time variant nature of the channel can be done by Doppler spread and coherence time. Coherence time, $T_c$, is the time over which the two received signals have strong potential for amplitude correlation [1]. Depending on how long the coherence time is in comparison with the symbol duration, $T_s$, a fading channel can be categorized either as time flat (slow fading) or time selective (fast fading). The fading is time flat if the symbol duration is much less than the channel coherence time, i.e., $T_s << T_c$. The channel is time selective if $T_s > T_c$. In this case the channel changes over duration of one symbol period with high probability, which leads to distortion of the baseband pulse shape and irreducible error rate.

It is noted that frequency selectivity and time selectivity are two different properties of a fading channel. Taking into account combinations of time selectivity and frequency selectivity, fading channels are conventionally divided into one of the following four types,

- Flat fading channels (time and frequency flat)
- Frequency selective fading channels (frequency selective but time flat)

- Time selective fading channels (time selective but frequency flat)
- Doubly selective fading channels (both frequency and time selective).

## 2.2 The MIMO Channel Model

For a MIMO system with $M_T$ transmit and $M_R$ receive antennas, consider the system model given in Figure 2.1. It should be noted that the multiple transmit and receive antennas could belong to a single user modem or it could be distributed among different users or base stations for distributed MIMO configuration and cooperative communications.

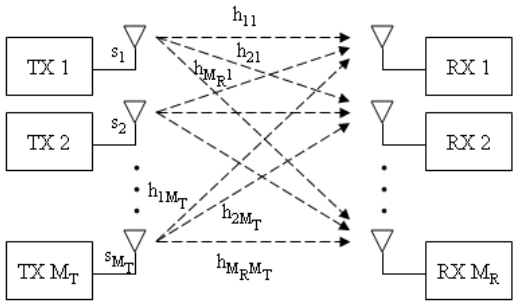


Figure 2.1: The MIMO channel.

At a certain time, assume that the $K\times 1$ modulated complex data symbols, $\mathbf{s} = [s_1, s_2, ..., s_K]^T$, are mapped into a transmit vector consisting of complex symbols $\mathbf{c} = [c_1, c_2, ..., c_{M_T}]^T$. Note that $K$ is not necessarily equal to $M_T$. The transmit vector $\mathbf{c}$ is transmitted simultaneously from the $M_T$ transmit antennas. The received signal at antenna $i$ can be expressed as,

$$y_i = \sum_{j=1}^{M_T} h_{ij}c_j + n_i, \tag{2.3}$$

where $h_{ij}$ is the channel coefficient from the $j^{th}$ transmit antenna to the $i^{th}$ receive antenna and the additive noise $n_i$ is a zero-mean complex Gaussian random variable with variance $N_0/2$ per dimension. Combining the received signals in a vector $\mathbf{y} = [y_1, y_2, ..., y_{M_R}]^T$, (2.3) becomes

$$\mathbf{y} = \mathbf{Hc} + \mathbf{n}, \tag{2.4}$$

where $\mathbf{n} = [n_1, n_2, ..., n_{M_R}]^T$ and $\mathbf{H}$ is the $M_R \times M_T$ channel matrix which can be expressed as,

$$\mathbf{H} = \begin{bmatrix} h_{11} & h_{12} & \cdots & h_{1M_T} \\ h_{21} & h_{22} & \cdots & h_{2M_T} \\ \vdots & \vdots & \ddots & \vdots \\ h_{M_R1} & h_{M_R2} & \cdots & h_{M_RM_T} \end{bmatrix}. \tag{2.5}$$

Note that this system model assumes that the channel undergoes flat fading and that the channel coefficients remain constant during the transmission of the symbol vector $\mathbf{c}$.

## 2.3 Diversity Techniques

The most effective technique to combat fading relies on the exploitation of diversity. In this section, we will discuss diversity techniques in space, time and frequency.

Time diversity can be achieved by transmitting the same messages in different time slots where the separation between the time interval is at least equal to the coherence time $T_c$ of the channel. Time diversity can be provided by combining error control coding with interleaving where the replicas of the transmitted signals are usually provided to the receiver in the form of redundancy in the time domain introduced by error control coding [39].

Depending on whether multiple antennas are used for transmission or reception, two types of spatial diversity become available: receive-antenna diversity and transmit-antenna diversity. It should be noted that the multiple antennas must be physically separated by a proper distance so that the individual signals are uncorrelated. In receive diversity, multiple antennas are deployed at the receiver to acquire independently faded copies of the transmitted signals which are then properly combined to mitigate channel fading to increase the overall received SNR.

Transmit diversity relies on multiple antennas at the transmitter. Transmit-antenna diversity schemes, can be divided into two categories: open loop and closed loop schemes. Closed loop schemes require channel knowledge at the transmitter, which is typically acquired through feedback channels. Although

feedback channels are present in most wireless systems, mobility may cause fast channel variations which cannot be tracked accurately by the transmitter.

Frequency diversity can be obtained via the frequencies separated by at least the coherence bandwidth of the channel and the frequencies are almost independent of each other. In wireless communications, the replicas of the transmitted signals are usually provided to the receiver in the form of redundancy in the frequency domain introduced by a multicarrier modulation such as OFDM, which will be discussed in detail in Chapter 3.

## 2.4 Space-Time Coding

In space-time (ST) coding joint encoding across multiple transmit antennas is carried out in order to maximize the reliability of a wireless link. ST coding schemes exploit spatial diversity in order to provide diversity and/or coding gains over an uncoded wireless link [6, 7].

The concept of ST coding was first introduced and the design criteria were established in [6]. In this section we will review these criteria.

### 2.4.1 ST Code Design

Consider the space-time coded system with $M_T$ transmit and $M_R$ receive antennas where the transmitted data is encoded by a space-time encoder. The data symbol vector $\mathbf{s} = [s_1, s_2, ..., s_K]^T$ is fed to the space-time encoder which maps it to the $M_T \times U$ codeword matrix

$$\mathbf{C} = \begin{bmatrix} c_1^1 & c_1^2 & \cdots & c_1^U \\ c_2^1 & c_2^2 & \cdots & c_2^U \\ \vdots & \vdots & \ddots & \vdots \\ c_{M_t}^1 & c_{M_t}^2 & \cdots & c_{M_t}^U \end{bmatrix} = \left[\mathbf{c}^1 \mathbf{c}^2 \cdots \mathbf{c}^U\right], \tag{2.6}$$

where $M_T$ symbols $\mathbf{c}^t = [c_1^t c_2^t \cdots c_{M_T}^t]^T$ are transmitted simultaneously from the transmit antennas for time instant $t = 1, 2, ..., U$. The design criteria are derived by characterizing the error probability, which is the probability that the transmitted codeword $\mathbf{C}$ is erroneously decided as another codeword $\mathbf{E} = \left[\mathbf{e}^1 \mathbf{e}^2 \cdots \mathbf{e}^U\right]$

by the receiver where $\mathbf{e}^t = \left[e_1^t e_2^t \cdots e_{M_T}^t\right]^T$ and

$$\mathbf{E} = \begin{bmatrix} e_1^1 & e_1^2 & \cdots & e_1^U \\ e_2^1 & e_2^2 & \cdots & e_2^U \\ \vdots & \vdots & \ddots & \vdots \\ e_{M_T}^1 & e_{M_T}^2 & \cdots & e_{M_T}^U \end{bmatrix}. \tag{2.7}$$

This is called the pairwise error probability (PEP) and is bounded by

$$P(\mathbf{C} \to \mathbf{E}|h_{ij}, i = 1, ..., M_R, j = 1, ..., M_T) \leq Q\left(\sqrt{\frac{E_s}{2N_0} d^2(\mathbf{C}, \mathbf{E}|\mathbf{H})}\right), \tag{2.8}$$

where $E_s$ is the average energy of data symbols and $\sqrt{E_s} = 1$ since the data symbols are chosen from a constellation with the average energy of elements equal to 1. This is a generally applied rule such that fair comparisons can be made when analyzing the performance of different constellations such as QPSK or 16-QAM. By noting that $Q(x) \leq \mathrm{e}^{-x^2/2}$, (2.8) becomes

$$P(\mathbf{C} \to \mathbf{E}|h_{ij}, i = 1, ..., M_R, j = 1, ..., M_T) \leq \exp(-d^2(\mathbf{C}, \mathbf{E}|\mathbf{H}) E_s / 4N_0), \tag{2.9}$$

where the Euclidean distance can be expressed as

$$d^2(\mathbf{C}, \mathbf{E}|\mathbf{H}) = \|\mathbf{H}(\mathbf{C} - \mathbf{E})\|_F^2 = \sum_{i=1}^{M_R} \sum_{t=1}^{U} \left| \sum_{j=1}^{M_T} h_{ij}(c_j^t - e_j^t) \right|^2. \tag{2.10}$$

It should be noted that the channel coefficients $h_{ij}$ are assumed to remain constant during the transmission of the $M_T \times U$ space-time code (STC) matrix.

We can define the codeword difference matrix $\mathbf{B} = (\mathbf{C} - \mathbf{E})$,

$$\mathbf{B} = (\mathbf{C} - \mathbf{E}) = \begin{pmatrix} c_1^1 - e_1^1 & c_1^2 - e_1^2 & \cdots & c_1^U - e_1^U \\ c_2^1 - e_2^1 & c_2^2 - e_2^2 & \cdots & c_2^U - e_2^U \\ \vdots & \vdots & \ddots & \vdots \\ c_{M_T}^1 - e_{M_T}^1 & c_{M_T}^2 - e_{M_T}^2 & \cdots & c_{M_T}^U - e_{M_T}^U \end{pmatrix}. \tag{2.11}$$

Therefore the code distance matrix can be defined as $\mathbf{A} = \mathbf{B}\mathbf{B}^H$. Noting that $\mathbf{h}_i = (h_{i1}, \cdots, h_{iM_T})$, (2.10) can also be written as

$$d^2(\mathbf{C}, \mathbf{E}|\mathbf{H}) = \sum_{i=1}^{M_R} \mathbf{h}_i \mathbf{A} \mathbf{h}_i^H. \tag{2.12}$$

$\mathbf{A}$ is a nonnegative definite Hermitian matrix since $\mathbf{A} = \mathbf{A}^H$and the eigenvalues of $\mathbf{A}$ are nonnegative real numbers [40]. Therefore there exists a unitary

matrix $\mathbf{V}$ and a real diagonal matrix $\mathbf{D}$ such that $\mathbf{VAV}^H = \mathbf{D}$. The eigenvalues $(\lambda_1\lambda_2\cdots\lambda_{M_t})$ of the matrix $\mathbf{A}$ are the diagonal entries of the matrix $\mathbf{D}$. Furthermore, by letting $(\beta_{i1},\cdots,\beta_{iM_t}) = \mathbf{h}_i\mathbf{V}^H$, it can be seen that

$$\mathbf{h}_i\mathbf{A}\mathbf{h}_i^H = \sum_{j=1}^{M_T} \lambda_j \left|\beta_{ij}\right|^2. \tag{2.13}$$

Since $\mathbf{V}$ is unitary, the rows $\{v_1, v_2, \cdots, v_{M_T}\}$ are the eigenvectors of $\mathbf{A}$ and are a complete orthogonal basis of $\mathbb{C}^{M_T}$. Substituting (2.13) in (2.12) and further substituting in (2.9) we obtain

$$P(\mathbf{C}\to\mathbf{E}|\mathbf{H}) \le \exp\left(-\frac{E_s}{4N_0}\sum_{i=1}^{M_R}\sum_{j=1}^{M_T}\lambda_j\left|\beta_{ij}\right|^2\right), \tag{2.14}$$

$$= \prod_{i=1}^{M_R}\exp\left(-\frac{E_s}{4N_0}\sum_{j=1}^{M_T}\lambda_j\left|\beta_{ij}\right|^2\right). \tag{2.15}$$

It can be seen that the upper bound on the conditional pairwise error probability expressed in (2.15) is a function of $|\beta_{ij}|$. The distribution of $|\beta_{ij}|$ can be determined with the knowledge of $h_{ij}$. $\mathbf{h}_i = (h_{i1},\cdots,h_{iM_T})$ are zero mean complex Gaussian random variables with variance 0.5 per dimension, therefore they are also Rayleigh distributed with probability density function (pdf)

$$p(|\beta_{ij}|) = 2\left|\beta_{ij}\right|\exp(-\left|\beta_{ij}\right|^2). \tag{2.16}$$

To find the upper bound on the average probability of error, (2.15) must be averaged with respect to the independent Rayleigh distribution of $|\beta_{ij}|$. The PEP was bounded in [6] as

$$P(\mathbf{C}\to\mathbf{E}) \le \left(\prod_{j=1}^{r}\lambda_j\right)^{-M_R}(E_s/4N_0)^{-rM_R}. \tag{2.17}$$

If we denote the nonzero eigenvalues of $\mathbf{A}$ by $(\lambda_1\lambda_2\cdots\lambda_r)$, where $r$ $(r \le M_T)$ is the rank of matrix $\mathbf{A}$, from (2.17), it can be seen that a diversity gain of $rM_R$ can be achieved. The diversity gain determines the exponential decay of the error rate versus SNR (the asymptotic slope of the performance curve on a log-log scale). It determines the approximate power gain of the system compared to a system with no diversity at the same error probability. Furthermore, from

(2.17) the achievable coding gain is $(\lambda_1\lambda_2\cdots\lambda_r)^{1/r}$. The coding gain determines the horizontal shift of the PEP curve for a coded system relative to an uncoded system with the same diversity gain.

In summary, given the codewords $\mathbf{C}$ and $\mathbf{E}$, the diversity order and coding gain must be maximized and the following criterion are established to this end.

**The Rank Criterion:** The diversity gain was shown to be $rM_R$ where $r$ is the minimum rank of the matrix $\mathbf{B}$ over all possible codeword pairs. Therefore to maximize the diversity gain $\mathbf{B}$ must be full rank which implies that $r$ must be maximized, i.e $r = M_T$. Then the maximum achievable diversity order is $M_T M_R$. The diversity gain determines the slope of the mean PEP versus SNR curve.

**The Determinant Criterion:** The coding gain is given by the minimum product of the nonzero eigenvalues of $\mathbf{B}$ over all distinct pairs of codewords. Since the product of the eigenvalues equals the determinant when the matrix is of full rank, this criterion is called the determinant criterion. The coding gain does not affect the asymptotic slope but results in a shift of the performance curve.

The ST coding schemes introduce temporal and spatial correlation into the signals transmitted from different antennas without increasing the total transmitted power or the transmission bandwidth. There is a diversity gain that results from the multiple paths between the base station and user terminal, and a coding gain that results from how symbols are correlated across transmit antennas. To minimize the PEP, both diversity gain and coding gain must be maximized. However since the diversity gain is an exponent in the upper bound in (2.17), it can be seen that at high SNR the diversity gain will dominate the PEP expression.

### 2.4.2 The Alamouti scheme

As mentioned in Chapter 1, in [7] Alamouti proposed a simple transmit and receive diversity scheme with linear ML decoding. The proposed ST code matrix is given as

$$\mathbf{C} = \begin{bmatrix} s_1 & -s_2^* \\ s_2 & s_1^* \end{bmatrix}, \tag{2.18}$$

where the column index indicates time and the row index indicates transmit antenna.

At the first signaling interval $t_1$, data symbols $s_1$ and $s_2$ are sent through the 2 transmit antennas and at the second signaling interval $t_2$, $s_2^*$ and $-s_1^*$ are sent. It can be seen that the code structure is orthogonal. Without loss of generality, let us assume that $M_R = 2$. At the receive antennas, the received signals at time $t_1$ are

$$\begin{aligned} y_{11} &= h_{11}s_1 + h_{12}s_2 + n_{11}, \\ y_{21} &= h_{21}s_1 + h_{22}s_2 + n_{21}, \end{aligned} \tag{2.19}$$

and at time $t_2$

$$\begin{aligned} y_{12} &= -h_{11}s_2^* + h_{12}s_1^* + n_{12}, \\ y_{22} &= -h_{21}s_2^* + h_{22}s_1^* + n_{22}, \end{aligned} \tag{2.20}$$

where $y_{ij}$ represents the received signal at receive antenna $i$ at time index $j$. The noise samples are independent and identically distributed (i.i.d.) complex Gaussian zero-mean random variables with variance $N_0/2$ per dimension. The receiver then computes the following estimates for $s_1$ and $s_2$,

$$\begin{aligned} \hat{s}_1 &= h_{11}^* y_{11} + h_{12} y_{12}^* + h_{21}^* y_{21} + h_{22} y_{22}^*, \\ \hat{s}_1 &= \left(|h_{11}|^2 + |h_{12}|^2 + |h_{21}|^2 + |h_{22}|^2\right) s_1 + h_{11}^* n_{11} + h_{12} n_{12}^* + h_{21}^* n_{21} + h_{22} n_{22}^*, \end{aligned} \tag{2.21}$$

and

$$\begin{aligned} \hat{s}_2 &= h_{12}^* y_{11} - h_{11} y_{12}^* + h_{22}^* y_{21} - h_{21} y_{22}^*, \\ \hat{s}_2 &= \left(|h_{11}|^2 + |h_{12}|^2 + |h_{21}|^2 + |h_{22}|^2\right) s_2 + h_{12}^* n_{11} - h_{11} n_{12}^* + h_{22}^* n_{21} - h_{21} n_{22}^*. \end{aligned} \tag{2.22}$$

It can be seen that this transmission scheme benefits from $4^{\,th}$ order diversity. Since this scheme transmits two symbols in two time slots, the rate of code is 1 symbol/per channel use (pcu) so that diversity gain is achieved without loss in bandwidth efficiency. Alamouti's scheme works only for the two transmit antenna case when complex symbols are used. There are no full rate space-time block code matrices for more than two transmit antennas when complex symbols are used. Tarokh et al. provided examples of lower rate code matrices that provide full diversity when complex symbols are used [8].

## 2.5 Spatial Multiplexing

Spatial multiplexing (SM) is a MIMO transmission technique which offers a linear increase in the transmission rate for the same bandwidth with no additional

power expenditure. In a SM scheme with $M_T = 2$, the original bit stream is split into two streams, which are modulated and transmitted simultaneously from both the antennas. For proper detection, the receiver must have perfect knowledge of the channel. Since the receiver has knowledge of the channel it provides receive diversity, but the system has no transmit diversity because streams transmitted over different antennas are completely different from each other since they carry different data. This way we can sacrifice transmit diversity to achieve higher throughput and incorporate diversity at the receiver in terms of receive diversity.

Here we consider a 2×2 MIMO system employing SM. At a certain time the data symbols $(s_1, s_2)$ are transmitted from the 2 transmit antennas simultaneously. The signals received by the two receive antennas are

$$\begin{aligned} y_1 &= h_{11}s_1 + h_{12}s_2 + n_1, \\ y_2 &= h_{21}s_1 + h_{22}s_2 + n_2. \end{aligned} \tag{2.23}$$

The maximum likelihood (ML) detector makes an exhaustive search over all possible values of the transmit symbol pair and decides in favor of $(\hat{s}_1, \hat{s}_2)$ which minimizes the Euclidean distance

$$D\left(\hat{s}_1, \hat{s}_2\right) = \left\{ |y_1 - h_{11}\hat{s}_1 - h_{12}\hat{s}_2|^2 + |y_2 - h_{21}\hat{s}_1 - h_{22}\hat{s}_2|^2 \right\}. \tag{2.24}$$

The minimization of the above metric requires an exhaustive search among the $|\mathcal{M}|^2$ possible transmitted signal vectors, where $|\mathcal{M}|$ is the signal constellation size. Therefore the complexity grows exponentially with the size of the constellation. Receiver decoding complexity is an important issue since we desire simple structures at the receiver.

# Chapter 3

# MIMO-OFDM and Performance of WiMAX PHY Layer

In this chapter we will first introduce the concept of OFDM and MIMO-OFDM. These schemes are extensively used in the IEEE 802.16 (WiMAX) standard which will be discussed in this chapter with an emphasis on the physical (PHY) layer. We will also discuss some ST coding schemes considered in WiMAX in addition to some space-frequency (SF) coding schemes which have been shown to be promising techniques but are not yet part of the standards. By making use of the threaded algebraic space-time (TAST) code framework we propose a SF coding scheme. We conclude the chapter by analyzing the performance of the WiMAX PHY layer and some ST and SF codes.

## 3.1 Orthogonal Frequency Division Multiplexing

As outlined in Chapter 2, systems which employ a large transmission bandwidth are affected by channel frequency selectivity. Traditional single carrier systems transmitting over frequency selective channels are affected by ISI which severely degrades performance and limits the transmission rate, unless complicated equalization techniques are employed.

Orthogonal frequency division multiplexing (OFDM) is a bandwidth efficient, multicarrier transmission technique which is tolerant to channel disturbances

such as multipath fading. In OFDM, a high rate serial data stream is split up into a parallel set of low-rate substreams which are simultaneously transmitted, then recombined at the receiver into a single high rate stream. Each substream is modulated on a separate subcarrier. By lowering the rate of the stream, the symbol duration is increased so that it is longer compared to the delay spread of the time-dispersive channel. Also since the rate of each stream is lower, the bandwidth of the subcarriers is decreased so that it is small compared with the coherence bandwidth of the channel, therefore the individual subcarriers experience flat fading. Thus OFDM converts a frequency selective fading channel into a set of parallel flat fading channels.

Using OFDM the channel is converted into a number of overlapping but mutually orthogonal subchannels in the frequency domain which do not interfere with each other. Therefore simultaneous transmission is possible without intercarrier interference (ICI). The subcarriers must overlap to ensure high spectral efficiency and it is still possible to recover the individual subcarriers despite their overlapping spectrum provided that the orthogonality is maintained. The orthogonality is achieved by making use of fast Fourier transform (FFT) algorithm. In the frequency domain, the subcarriers have a *sinc* pulse shape such that the main lobe of each subcarrier lies on the nulls of all other subcarriers thereby avoiding ICI. The frequency spectrum of an OFDM signal with 1 MHz subcarrier spacing is shown in Figure 3.1.

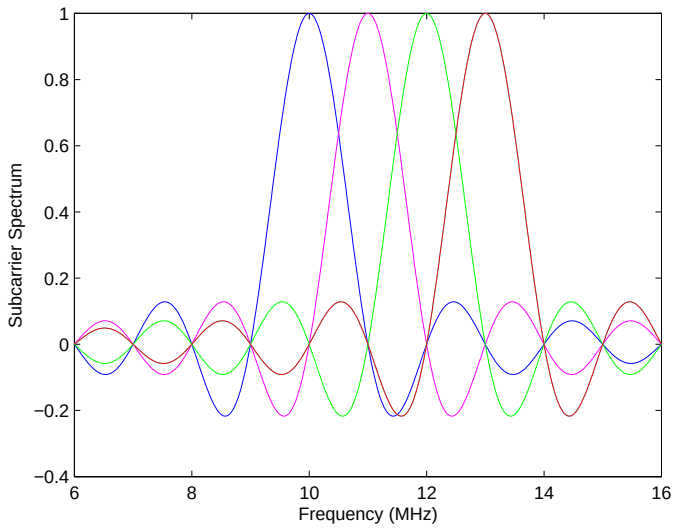


Figure 3.1: Overlapping subcarriers in an OFDM system.

OFDM can be easily implemented by using the FFT algorithm. At the transmitter an OFDM system treats the source symbols as though they were in the frequency domain and feeds the symbols to an inverse fast Fourier transform (IFFT) block which brings the signal into the time domain and modulates the data onto orthogonal subcarriers. Let $N$ be the number of carriers available in the OFDM system and one PSK or QAM symbol is transmitted per subcarrier. The OFDM symbol is the superposition of $N$ subcarriers spaced $\Delta f = 1/T_0$ Hz apart where $T_0$ is the OFDM symbol duration. The time domain OFDM symbol is given as,

$$q_n = \frac{1}{\sqrt{N}} \sum_{k=0}^{N-1} s_k e^{\frac{j2\pi kn}{N}}, \quad n = 0, ..., N-1, \tag{3.1}$$

where it can be seen that the symbol $s_k$ modulates a complex sinusoid. Note that the scaling factor $1/\sqrt{N}$ is included so that the average power of $q_n$'s equals that of $s_k$'s.

After the IFFT operation, a cyclic prefix (CP) is added to the beginning of each OFDM symbol which is transmitted before the actual OFDM symbol itself. CP is a copy of the last part of the OFDM symbol, and it extends the length of the transmitted signal and guards the symbol by being interfered from delayed copies of the previous symbols. The CP is illustrated in Figure 3.2. The total duration of the symbol can be written as $T_S = T_0 + T_{CP}$, where $T_S$ is the total duration of the transmitted symbol, $T_0$ is the duration of the OFDM symbol after IFFT operation and $T_{CP}$ is the duration of the CP.

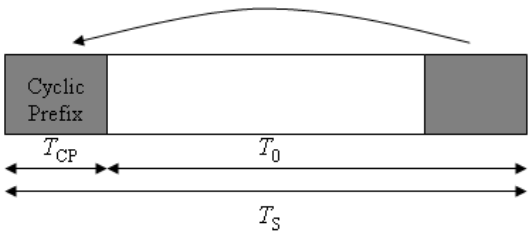


Figure 3.2: Addition of the cyclic prefix to an OFDM symbol.

The length of the CP should be greater than the maximum excess delay of the multipath channel. The CP is removed at the receiver and different subcarriers can be separated by passing them through an FFT block, therefore bringing them back to the frequency domain. Due to the CP, the linear convolution of the

channel impulse response with the transmitted data becomes a cyclic convolution. Due to the properties of cyclic convolution, the effect of the multipath channel is converted to a pointwise multiplication of the transmitted data symbols by the channel transfer function. Therefore by using CP, ISI is completely eliminated from the system.

When there is high mobility, i.e., high Doppler spread in the system such that the channel becomes a time-variant channel, the variations disrupt the orthogonality of the subcarriers and cause ICI. In those cases, a more complex system is needed to model such behavior. The effects of mobility on system performance will be investigated in Section 3.5. For low mobility cases when there exists insignificant Doppler spread, ICI may be ignored.

OFDM can be easily utilized for multiple access purposes. Orthogonal Frequency Division Multiple Access (OFDMA) is based on OFDM and it is implemented by dividing the total bandwidth into a number of subchannels consisting of a set of subcarriers. Users may occupy one or more than one subchannel, depending on their quality of service (QoS) requirements and the system loading characteristics. There are two strategies for allocating subcarrier groups to users. The first strategy groups adjacent subcarriers in the same frequency range in each subchannel. In the second one, the subchannels are spread over the total bandwidth. These subchannelization schemes will be further discussed in Section 3.3.

## 3.2 MIMO-OFDM

In a MIMO-OFDM system, the MIMO channels on each subcarrier can be modeled similar to the MIMO channel for single carrier systems except that now the channel is frequency selective with $L$ distinct paths. From Chapter 2, (2.1) can be extended to a MIMO system with $M_T$ transmit and $M_R$ receive antennas. For simplicity it is assumed that the channel is time-invariant for the duration of one OFDM symbol but may change from symbol to symbol. This change may be the result of mobility present in the channel and the channel variations with respect to OFDM symbol index $u$ may be rapid or slow depending on the mobility. The channel impulse response from transmit antenna $j$ to receive antenna $i$,

at OFDM symbol index $u$ can be expressed as

$$h_{ij}^{u}(\tau) = \sum_{l=0}^{L-1} \alpha_{ij}^{u}(l)\delta(\tau - \tau_l), \tag{3.2}$$

where $\alpha_{ij}^{u}(l)$ is the complex amplitude of the $l^{\text{th}}$ path from transmit antenna $j$ to receive antenna $i$ with time delay $\tau_l$. It should be noted that the $\alpha_{ij}^{u}(l)$'s describe the small-scale fading in the channel therefore path loss and log normal shadowing effects are ignored. The $\alpha_{ij}^{u}(l)$'s are zero-mean, complex Gaussian random variables which are independent for any $(i, j, l, u)$. It is also assumed that the path gains between any transmit and receive antenna pair follow the same power delay profile such that $E[|\alpha_{ij}^{u}(l)|^2] = \beta_l^2$ for all $(i, j, l, u)$. The powers of the $L$ paths are normalized such that $\sum_{l=0}^{L-1} \beta_l^2 = 1$. This normalization is important because it ensures that the received power at each receive antenna is equal to total transmitted power.

The frequency response of the channel for the $k^{\text{th}}$ subcarrier during the $u^{\text{th}}$ OFDM symbol is

$$\tilde{H}_{ij}^{u}(k) = \sum_{l=0}^{L-1} \alpha_{ij}^{u}(l)e^{-j2\pi k\Delta f\tau_l}, \tag{3.3}$$

$$= \sum_{l=0}^{L-1} \alpha_{ij}^{u}(l)e^{-j2\pi kl/N}. \tag{3.4}$$

Using this we can express the received signal after CP removal and FFT operations by noting that due to the use of the CP, the received signal is the pointwise multiplication of the transmitted symbols by the channel frequency response. The received signal at receive antenna $i$ on the $k^{\text{th}}$ subcarrier at OFDM symbol index $u$ is given by

$$y_i^u(k) = \frac{1}{\sqrt{M_T}} \sum_{j=1}^{M_T} \tilde{H}_{ij}^{u}(k)s_j^u(k) + v_i(k), \tag{3.5}$$

where $v_i(k)$ is the additive complex Gaussian noise which is assumed to be i.i.d. circularly symmetric with variance $N_0/2$ per dimension. It should be noted that the noise process, $n$, acting on the original received signal before CP removal and FFT operations, becomes the noise process $v$ after CP removal and FFT. Therefore the noise process $v$ is basically the FFT of the noise process $n$. However,

due to the special structure of the FFT matrix, the distribution of the noise processes are the same [14]. The $\frac{1}{\sqrt{M_T}}$ factor is included so that the total transmitted power is constrained to 1, regardless of the number of transmit antennas $M_T$. It is assumed that the signals transmitted from individual antenna elements have equal powers of $\frac{1}{\sqrt{M_T}}$ such that the transmit power is distributed equally across all antennas.

## 3.3 IEEE 802.16 PHY Layer

The IEEE 802.16 standard is considered as a solution for future wireless broadband communications that offer high data rates, more scalability, broader coverage. Worldwide Interoperability for Microwave Access, known as WiMAX, is a wireless networking standard which aims to provide conformance and interoperability across IEEE 802.16 standard based products. In this section we will review the physical (PHY) layer of the IEEE 802.16 standard which will serve as the basis of our simulations. Several other amendments are still under development addressing issues such as advanced air interface [41] and we will also consider some new techniques put forth in this amendment. For the rest of this thesis, the term WiMAX and IEEE 802.16 will be used interchangeably.

The IEEE 802.16 standard is a family of standards. The latest IEEE 802.16e-2005 is an evolution from the IEEE 802.16d-2004 standard which merged and revised all the earlier versions of the standard. We will use the configurations specified in IEEE 802.16e in the rest of this work. The IEEE 802.16e air interface adopts OFDMA for improved multipath performance in non-line-of-sight (NLOS) environments. Scalable OFDMA is also introduced to support scalable channel bandwidths from 1.25 to 20 MHz which allows the data rate to scale easily by choosing a different FFT size based on the available channel bandwidth.

The PHY layer includes forward error correction (FEC), constellation mapping (modulation), ST coding, subcarrier permutation and OFDM on the transmitter side and recovery operations on the receiver side that are the reverse of the operations carried out at the transmitter. A block diagram of the WiMAX PHY layer is shown in Figure 3.3. The receiver also includes channel estimation and carrier frequency synchronization blocks which are omitted here since throughout this work perfect channel estimation and synchronization is assumed. Furthermore, we will be studying the downlink only.

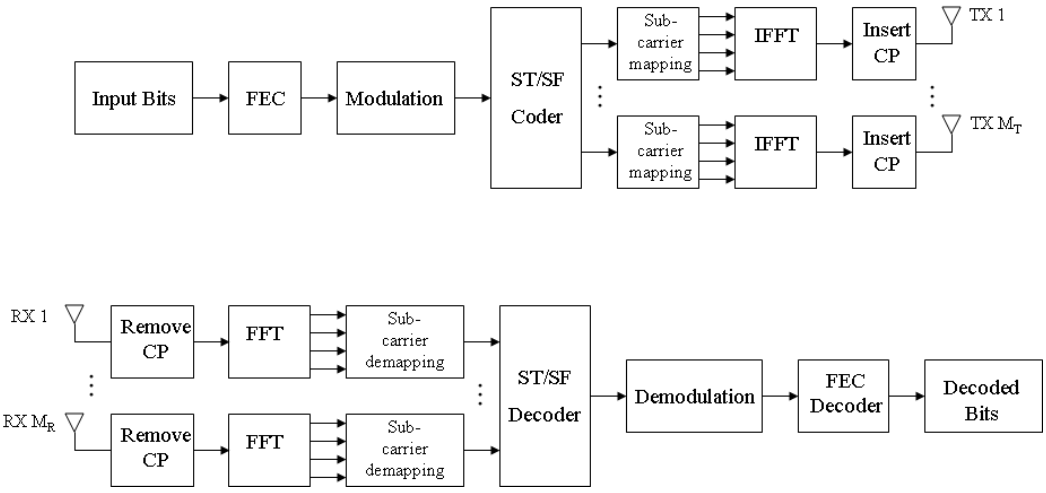


Figure 3.3: Block diagram of WiMAX PHY layer.

The data bits are first passed through a FEC block which consists of channel coding and interleaving. Channel coding is the process of adding redundant information bits into a data block for error-detection and correction purposes, where the amount of redundancy will determine the robustness of the transmission to impairments. Several different encoding schemes are present in the standard however we will consider convolutional codes (CC) and convolutional turbo codes (CTC) in this thesis.

Interleaving is a deterministic process which changes the order of transmitted bits. It is used to prevent long error bursts and therefore reduce the error concentration to be corrected. For OFDM systems, this means that bits that were adjacent in time are transmitted on subcarriers that are spaced out in frequency. In WiMAX, interleaving is done through a two stage permutation, the first is to avoid mapping adjacent coded bits on adjacent sub-carriers and the second permutation insures that adjacent coded bits are mapped alternately onto less or more significant bits of the constellation, thus avoiding long runs of unreliable bits.

Once the signal has been FEC coded, it enters the modulation block where the bits are Gray coded into symbols. To achieve equal average symbol energy, the constellations are normalized by multiplying all of its points by an appropriate factor. The next stage is ST or SF coding. Some of the schemes considered for this block will be discussed in detail in Sections 3.3.1 and 3.4.

After this, the next step is subchannelization. In OFDMA, the resource allocated to a user is called a subchannel. The formation of subchannels differ based on the permutation scheme in use. Here we will consider two subchannelization schemes. The first one is partial usage of subcarriers (PUSC) which assigns subcarriers that are distributed across the bandwidth to each subchannel. The second one is called band AMC and this scheme assigns contiguous subcarriers to each subchannel.

In PUSC the symbols are grouped together into slots, slots are grouped into clusters, pilot positions are determined, clusters are grouped into groups and subchannels are formed out of these groups. The end result is a burst unit which is several subcarriers wide and several symbols long and the subcarriers are not necessarily contiguous to each other. The pilot subcarriers are embedded in between the data subcarriers to provide channel state information (CSI) at the receiver. Regardless of the subchannelization scheme, guard subcarriers which are set to null are placed at the start and end of each symbol. The other subcarrier permutation scheme considered here is band AMC, in which subchannels are composed of adjacent subcarriers. Although OFDMA is intended for multiple users to be scheduled on the subchannels, we analyze the case where a single user occupies all available subchannels. This simplifying assumption is made so that we can better analyze the effects of other parameters, such as FEC coding or space-time coding, on the performance of the WiMAX PHY layer.

After the completion of these steps, the resulting signal is fed to the OFDM modulator and is ready to be transmitted through the $M_T$ transmit antennas. At the receiver the reverse operations are applied to decode the signal.

In WiMAX, there is a mechanism which adjusts modulation and coding parameters dynamically to maximize throughput and minimize bit error rate (BER) in the face of changing channel conditions which is called adaptive modulation and coding (AMC). The FEC profiles are paired with several modulation schemes to form burst profiles of varying robustness and efficiency. There are different block size and code rate options for the different modulation types. The users report their current channel condition to the BS and based on this feedback, a coding profile is selected for the downlink data transmissions. Thus, users who experience poor channel conditions, i.e., low SNR, at a given time, will be provided with better error correction than those users experiencing better channel conditions at the same time. In Section 3.5 we will analyze the performance of the WiMAX PHY layer for some of these FEC profiles.

### 3.3.1 MIMO Techniques in IEEE 802.16

The IEEE 802.16 standard defines some MIMO techniques in order to achieve transmit diversity and/or higher spectral efficiency. Although they are present in the 802.16e-2005 standard as optional features, it is clear that these techniques are essential for achieving the performance requirements since they can enhance transmission speed and/or reception quality of the signals. That's why WiMAX Forum has specified the Alamouti ST code and SM as two mandatory profiles for the downlink.

For $M_T = 2$ there are three MIMO techniques. They include the Alamouti ST code, SM and a variant of the Golden code which incorporates the benefits of ST codes and SM. The space-time code given in the standard is the Alamouti code, referred to as Matrix $\mathbf{A}$, and is given below. This code has a rate of 1 symbol/pcu. We will refer to this code as space-time Alamouti (ST-Alamouti) to avoid confusion with the code which will be presented in Section 3.4.

$$\mathbf{A} = \begin{bmatrix} \mathbf{s}_1 & -\mathbf{s}_2^* \\ \mathbf{s}_2 & \mathbf{s}_1^* \end{bmatrix}, \tag{3.6}$$

where the row index indicates the transmit antenna number and column index indicates the OFDM symbol. Here $\mathbf{s}_i$ contains only data symbols. Before OFDM transmission occurs, depending on the subchannelization scheme these data subcarriers will undergo a permutation scheme and the null and pilot subcarriers will be placed amongst the data subcarriers. Let *ncarr* be the number of data subcarriers in an OFDM symbol. We can express the data symbols within Matrix $\mathbf{A}$ as

$$\mathbf{A} = \begin{bmatrix} (s_1 \ s_3 \dots s_{2ncarr-1}) & -(s_2^* \ s_4^* \dots \ s_{2ncarr}^*) \\ (s_2 \ s_4 \dots \ s_{2ncarr}) & (s_1^* \ s_3^* \dots s_{2ncarr-1}^*) \end{bmatrix}, \tag{3.7}$$

where the data symbols will be input to the subcarrier mapping block, where if PUSC is used as the subcarrier mapping scheme they will be reordered and distributed across the OFDM symbol. If AMC is used they will be mapped contiguously. After mapping has taken place, pilot subcarriers will be inserted among the data subcarriers and guard subcarriers will be placed at the beginning and end of the OFDM symbol. These steps will be carried out for all of the ST code and SM matrices given below.

The other ST code is Matrix $\mathbf{C}$ which is a variant of the Golden code presented in [10]. This code has a decoding complexity of $|\mathcal{M}|^4$ for $\mathcal{M}$-ary data symbols.

The Golden code combines diversity gain and multiplexing gain to achieve a rate of 2 symbols/pcu, which is twice the rate of Matrix **A**. Again for this code, and for the rest of the codes mentioned in this section, the row index indicates the transmit antenna number and column index indicates the OFDM symbol. We omit the data mappings for Matrix **C** since it is straightforward to apply the technique given in (3.7).

$$\mathbf{C} = \frac{1}{\sqrt{1+r^2}} \begin{bmatrix} \mathbf{s}_1 + jr\mathbf{s}_4 & r\mathbf{s}_2 + \mathbf{s}_3 \\ \mathbf{s}_2 - r\mathbf{s}_3 & jr\mathbf{s}_1 + \mathbf{s}_4 \end{bmatrix}, \quad r = \frac{-1+\sqrt{5}}{2}. \tag{3.8}$$

The pure SM method, which also achieves a rate of 2 symbols/pcu but with no transmit diversity, is given in Matrix **B**. The SM matrix does not have a time index such that all of the symbols are sent within one OFDM symbol.

$$\mathbf{B} = \begin{bmatrix} \mathbf{s}_1 \\ \mathbf{s}_2 \end{bmatrix}, \tag{3.9}$$

where the data symbols within Matrix **B** are

$$\mathbf{B} = \begin{bmatrix} (s_1 \ s_3 \ \ldots s_{ncarr-1}) \\ (s_2 \ s_4 \ \ldots \ s_{ncarr}) \end{bmatrix}. \tag{3.10}$$

The transmission schemes for 4 BS transmit antennas also use the Alamouti code. If the desired rate is 1 symbol/pcu, the Alamouti code is used in blocks at only two antennas in an alternating fashion; and if the desired rate is 2 symbols/pcu, two Alamouti blocks are multiplexed using all four antennas. These schemes are also named Matrix **A** and Matrix **B**, respectively. The latter case obviously introduces interference between subcarriers. The data mappings for these matrices are carried out in a similar fashion to (3.7).

$$\mathbf{A} = \begin{bmatrix} \mathbf{s}_1 & -\mathbf{s}_2^* & 0 & 0 \\ \mathbf{s}_2 & \mathbf{s}_1^* & 0 & 0 \\ 0 & 0 & \mathbf{s}_3 & -\mathbf{s}_4^* \\ 0 & 0 & \mathbf{s}_4 & \mathbf{s}_3^* \end{bmatrix}. \tag{3.11}$$

$$\mathbf{B} = \begin{bmatrix} \mathbf{s}_1 & -\mathbf{s}_2^* & \mathbf{s}_5 & -\mathbf{s}_7^* \\ \mathbf{s}_2 & \mathbf{s}_1^* & \mathbf{s}_6 & -\mathbf{s}_8^* \\ \mathbf{s}_3 & -\mathbf{s}_4^* & \mathbf{s}_7 & \mathbf{s}_5^* \\ \mathbf{s}_4 & \mathbf{s}_3^* & \mathbf{s}_8 & \mathbf{s}_6^* \end{bmatrix}. \tag{3.12}$$

There also exists some variations to the 2 matrices above. These matrices have the same form as (3.11) and (3.12) but instead of 4 OFDM symbol durations, the coding is done across two OFDM symbols and two subcarriers. The first two columns refer to the first subcarrier over two OFDM symbols and the last two columns refer to the second subcarrier over two OFDM symbols. To illustrate data mappings in this case, coding across two OFDM symbols and two subcarriers for (3.11) results in

$$\begin{bmatrix} \overset{\rightarrow Subcarrier}{(s_1\ 0\ s_5\ 0 \ldots s_{2ncarr-3})} & \overset{\rightarrow Subcarrier}{(-s_2^*\ \ 0\ -s_6^*\ \ 0 \ldots -s_{2ncarr-2}^*)} \\ (s_2\ 0\ s_6\ 0 \ldots s_{2ncarr-2}) & (\ s_1^*\ \ 0\ \ s_5^*\ \ 0 \ldots\ s_{2ncarr-3}^*) \\ (0\ \ s_3\ 0\ s_7 \ldots s_{2ncarr-1}) & (\ 0 - s_4^*\ \ 0\ -s_8^* \ldots -s_{2ncarr}^*) \\ (0\ \ s_4\ 0\ s_8 \ldots s_{2ncarr}) & (\ 0\ \ s_3^*\ \ 0\ \ s_7^* \ldots\ s_{2ncarr-1}^*) \end{bmatrix}, \tag{3.13}$$

and for (3.12) we obtain

$$\begin{bmatrix} \overset{\rightarrow Subcarrier}{(s_1\ s_5\ s_9\ s_{13}\ \ldots s_{ncarr-3})} & \overset{\rightarrow Subcarrier}{(-s_2^*\ -s_7^*\ -s_{10}^*\ -s_{15}^* \ldots -s_{4ncarr-2}^*)} \\ (s_2\ s_6\ s_{10}\ s_{14} \ldots s_{ncarr-2}) & (\ s_1^*\ -s_8^*\ \ s_9^*\ \ -s_{16}^* \ldots -s_{4ncarr-3}^*) \\ (s_3\ s_7\ s_{11}\ s_{15} \ldots s_{ncarr-1}) & (-s_4^*\ \ s_5^*\ -s_{12}^*\ \ s_{13}^*\ \ldots\ \ s_{4ncarr}^*) \\ (s_4\ s_8\ s_{12}\ s_{16} \ldots s_{ncarr}) & (\ s_3^*\ \ s_6^*\ \ s_{11}^*\ \ s_{14}^*\ \ldots\ \ s_{4ncarr-1}^*) \end{bmatrix}. \tag{3.14}$$

Again the column index indicates the OFDM symbol and row index indicates the transmit antenna.

## 3.4 Space-Frequency Coding

In this section we investigate space-frequency (SF) coding for OFDM systems with multiple transmit antennas, where coding is applied in the frequency domain (OFDM carriers) rather than in the time domain (OFDM symbols).

SF coding basically extends the theory of ST coding for narrowband flat fading channels to broadband and frequency selective channels. The application

of classical space-time coding techniques for narrowband flat fading channels to OFDM seems straightforward, since the individual subcarriers can be seen as independently flat fading channels. However, in [18] it was shown that the design criteria for space-frequency codes operating in the space-time and frequency domain are different from those for classical space-time codes for narrowband fading channels as introduced in [6].

We briefly summarize the design criteria given in [18]. The derivation is similar to that given in Section 2.4.1 with the important exception that the channel is now a frequency selective channel and OFDM is employed. It is assumed that the orthogonality between the subcarriers is maintained. We must also modify $\mathbf{C}$ and $\mathbf{E}$ because the time index is now replaced with the subcarrier index. The symbols transmitted from the $M_T$ transmit antennas on the $k^{th}$ subcarrier is

$$\mathbf{c}_k = [c_k^1 c_k^2 \cdots c_k^{M_T}]^T,$$

with $c_k^j$ denoting the space-frequency coded symbol transmitted from the $j^{th}$ transmit antenna on the $k^{th}$ subcarrier. Again the design criteria are derived by characterizing the error probability, which is the probability that the transmitted codeword $\mathbf{C} = [\mathbf{c}_0 \mathbf{c}_1 \cdots \mathbf{c}_{N-1}]$ is erroneously decided as $\mathbf{E} = [\mathbf{e}_0 \mathbf{e}_1 \cdots \mathbf{e}_{N-1}]$

Therefore, (2.8) can be modified as

$$P(\mathbf{C} \to \mathbf{E}|\tilde{\mathbf{H}}(k)) = Q\left(\sqrt{\frac{E_s}{2N_0} d^2(C, E|\tilde{\mathbf{H}}(k))}\right), \tag{3.15}$$

where $\tilde{\mathbf{H}}(k)$ is the MIMO channel matrix for subcarrier $k$ with elements given in (3.4). We note that

$$d^2(\mathbf{C}, \mathbf{E}|\tilde{\mathbf{H}}(k)) = \sum_{k=0}^{N-1} \left\| \tilde{\mathbf{H}}(k)(\mathbf{c}_k - \mathbf{e}_k) \right\|_F^2 \tag{3.16}$$

is the Euclidean distance between $\mathbf{C}$ and $\mathbf{E}$ for the given channel. Again using the upper bound $Q(x) \leq \mathrm{e}^{-x^2/2}$, (3.15) becomes

$$P(\mathbf{C} \to \mathbf{E}|\tilde{\mathbf{H}}(k)) = \exp(-d^2(\mathbf{C}, \mathbf{E}|\tilde{\mathbf{H}}(k) E_s / 4N_0). \tag{3.17}$$

The expected pairwise error probability is found by averaging the conditional pairwise error probability bound in (3.16) over all channel realizations. For this we define $\mathbf{y}_k = \tilde{\mathbf{H}}(k)(\mathbf{c}_k - \mathbf{e}_k)$. The received signal is similar to (2.4) with the

exception that the subcarrier index $k$ has been added. We can define $\mathbf{Y} = [\mathbf{y}_0^T \mathbf{y}_1^T \cdots \mathbf{y}_{N-1}^T]$ so that $d^2(\mathbf{C}, \mathbf{E}|\tilde{\mathbf{H}}(k)) = \|\mathbf{Y}\|_F^2$ and (3.16) can be written as

$$P(\mathbf{C} \to \mathbf{E}|\tilde{\mathbf{H}}(k)) \leq \exp\left(-\frac{E_s}{4N_0}\|\mathbf{Y}\|_F^2\right). \tag{3.18}$$

$\mathbf{Y}$ is Gaussian since the $\alpha_{ij}$'s from which $\tilde{\mathbf{H}}(k)$ is computed are i.i.d Gaussian. The average of the conditional bound in (3.17) is fully characterized by the eigenvalues of the covariance matrix $\mathrm{Cov}(\mathbf{Y}) = \mathrm{E}\left\{\mathbf{Y}\mathbf{Y}^{\mathrm{H}}\right\}$ which is given as

$$\mathrm{Cov}(\mathbf{Y}) = \sum_{l=0}^{L-1}[(\mathbf{D}^l)(\mathbf{C}-\mathbf{E})^T(\mathbf{C}-\mathbf{E})^*(\mathbf{D}^l)^H] \otimes \mathbf{I}_{M_r}, \tag{3.19}$$

where $\mathbf{D}^l = diag\{e^{-j2\pi kl/N}\}_{k=0}^{N-1}$ and $\mathbf{I}_{M_r}$ is the correlation matrix of the channel. The superscript $^*$ denotes elementwise conjugation.

The rank of $\mathrm{Cov}(\mathbf{Y})$ can be written in terms of the rank of the $N \times N$ matrix

$$\mathbf{Z} = \sum_{l=0}^{L-1}[(\mathbf{D}^l)(\mathbf{C}-\mathbf{E})^T(\mathbf{C}-\mathbf{E})^*(\mathbf{D}^l)^H]. \tag{3.20}$$

This matrix can be decomposed as

$$\mathbf{Z} = \mathbf{F}(\mathbf{C}, \mathbf{E})\mathbf{F}^H(\mathbf{C}, \mathbf{E}), \tag{3.21}$$

where $\mathbf{F}(\mathbf{C}, \mathbf{E})$ is defined as

$$\mathbf{F}(\mathbf{C}, \mathbf{E}) = [(\mathbf{C}-\mathbf{E})^T \quad \mathbf{D}(\mathbf{C}-\mathbf{E})^T \quad \cdots \quad \mathbf{D}^{L-1}(\mathbf{C}-\mathbf{E})^T]. \tag{3.22}$$

The rank of $\mathrm{Cov}(\mathbf{Y})$ is $\mathrm{rank}(\mathrm{Cov}(\mathbf{Y})) = \mathrm{rank}(\mathbf{Z}) \times \mathrm{M_R}$. The diversity order can be determined by finding the minimum rank of the $N \times M_T L$ matrix $\mathbf{F}(\mathbf{C}, \mathbf{E})$ over the set of all distinct codewords $\mathbf{C}$ and $\mathbf{E}$. Of course the key assumption is that $N > M_t L$.

Therefore the maximum rank of $\mathbf{F}(\mathbf{C}, \mathbf{E})$ can be $M_T L$, which is established when $(\mathbf{C}-\mathbf{E})$ has rank $M_T$ for all distinct codewords $\mathbf{C}$ and $\mathbf{E}$ and each block $\mathbf{B}_i = \mathbf{D}^i(\mathbf{C}-\mathbf{E})^T$ is linearly independent of each other. When the linear independence of each block $\mathbf{B}_i$, $i = 0, \cdots, L-1$ , is satisfied the space frequency code exploits all the available frequency diversity.

If the SF code we are using is originally designed as a ST code for a single carrier narrowband system and it achieved diversity order $d$, then it will achieve

at least that same order in a broadband OFDM system. This can be proven by noting that if $(\mathbf{C}-\mathbf{E})$ has minimum rank $d$, then the minimum rank of $\mathbf{F}(\mathbf{C},\mathbf{E})$ will also be at least $d$ . Therefore it is possible to conclude that systems using ST codes directly as SF codes can achieve only full spatial diversity and are not guaranteed to achieve the full spatial and frequency diversity $M_t M_R L$.

With these in mind, besides coding the symbols in time and space, the new draft revision to the IEEE 802.16 standard supports a technique referred to as frequency hopping diversity coding (FHDC) for the downlink [41]. This technique is similar to Alamouti coding, but the OFDM symbol index is replaced by the subcarrier index, leading to coding in frequency and space. We will refer to this scheme as space-frequency Alamouti (SF-Alamouti). In SF-Alamouti, the Alamouti code matrix is applied across two adjacent subcarriers and thus within one OFDM symbol time. The mapping of the data symbols can be seen below, where again the row index represents transmit antenna number.

$$SFA = \begin{bmatrix} (s_1 - s_2^* \; s_3 \; - s_4^* \ldots s_{ncarr-1} - s_{ncarr}^*) \\ (s_2 \quad s_1^* \; s_4 \quad s_3^* \ldots \; s_{ncarr} \quad s_{ncarr-1}^*) \end{bmatrix}. \qquad (3.23)$$
$$\rightarrow Subcarrier$$

It should be noted that since coding is carried out across subcarriers, this scheme relies on the channel gains of adjacent subcarriers to be identical just as ST-Alamouti relies on the channel to stay constant for two signaling periods. By assuming that adjacent subcarriers have almost identical channel gains the linear complexity Alamouti decoding scheme may be applied across every received subcarrier pair with a possible loss in performance when the assumption does not hold. However we can ascertain the validity of our assumption by noting that the channel gain variations between subcarriers depend on the channel length, power delay profile and OFDM symbol length $N$. Since $N$ is typically large in IEEE 802.16 systems the channel variation between subcarriers is minimal and therefore does not have a severe effect in performance because of the finer partitioning of the frequency selective channel.

### 3.4.1 TAST Framework for SF Coding

The threaded algebraic space-time (TAST) code architecture combines spatial multiplexing and transmit diversity. It was proposed in [11]. The TAST architecture is a layered space time architecture which utilizes efficient algebraic code design.

As described in Section 3.3.1, when we use the Alamouti code multiplexed over 4 antennas to achieve a rate of 2 symbols/pcu there is interference. To avoid this interference and still achieve a rate 2 symbols/pcu code, we propose making use of the TAST code framework [11], which makes use of the layering concept. In this framework, symbols are separated into multiple threads and undergo a complex rotation after which they are multiplexed over space and time. We will apply this code to the frequency domain such that proposed code is shown in (3.24) for the first 4 subcarriers. The rest of the subcarriers are coded in a similar fashion. The TAST code given in [11] is

$$TAST = \begin{bmatrix} x_{11} & 0 & 0 & \phi^{1/4}x_{24} \\ \phi^{1/4}x_{21} & x_{12} & 0 & 0 \\ 0 & \phi^{1/4}x_{22} & x_{13} & 0 \\ 0 & 0 & \phi^{1/4}x_{23} & x_{14} \end{bmatrix} \begin{matrix} \downarrow Antenna, \\ \\ \\ \\ \rightarrow Subcarrier \end{matrix} \tag{3.24}$$

where $\phi = e^{j\pi/6}$ is the Diophantine number and

$$(x_{j1}, \ldots, x_{j4})^T = \mathbf{M}\,(s_{j1}, \ldots, s_{j4})^T, \quad j = 1, 2, \tag{3.25}$$

where $j$ denotes the layer index and the complex rotation matrix used here, which is given in [13], is

$$\mathbf{M} = \frac{1}{2}\begin{bmatrix} 1 & \theta & \theta^2 & \theta^3 \\ 1 & \theta & -\theta^2 & -\theta^3 \\ 1 & j\theta & -\theta^2 & -j\theta^3 \\ 1 & -j\theta & -\theta^2 & j\theta^3 \end{bmatrix}, \quad \theta = e^{j\pi/8}. \tag{3.26}$$

With the use of this rotation matrix, the output rotated symbols belonging to a thread contain information about all the data symbols within that thread. The

Diophantine number is used such that each thread belongs to a different algebraic subspace. This scheme relies on the joint detection of both layers, therefore (3.24) has a decoding complexity of $|\mathcal{M}|^8$, which is largely prohibitive.

### 3.4.2 A method for complexity reduction

To alleviate the decoding complexity we make use of the algorithm presented in [9], where the authors present a low complexity decoding scheme. We will briefly review this scheme here.

The space-time code matrix for a $2 \times 2$ single-carrier system used in the scheme proposed in [9] is given as

$$C = \begin{bmatrix} as_1 + bs_3 & -cs_2^* - ds_4^* \\ as_2 + bs_4 & cs_1^* + ds_3^* \end{bmatrix}, \tag{3.27}$$

where $a, b, c, d$ are complex-valued design parameters to be optimized under transmit power constraints and coding gain. Adopting the notation used in Section 2.4.2, the received signals can be written as

$$\begin{aligned} y_{i1} &= h_{i1}(as_1 + bs_3) + h_{i2}(as_2 + bs_4) + n_{i1}, \\ y_{i2} &= h_{i1}(-cs_2^* - ds_4^*) + h_{i2}(cs_1^* + ds_3^*) + n_{i2}, \end{aligned} \tag{3.28}$$

where $y_{ij}$ represents the received signal at receive antenna $i$ at time index $j$. The ML detector makes an exhaustive search over all the possible $|\mathcal{M}|^4$ quadruplets $(s_1, s_2, s_3, s_4)$ to decode the transmitted symbols. However, the special structure of this code allows for a simpler decoding scheme. This scheme involves the computation of some intermediate signals and recombining them such that the detection problem becomes decoupled. To achieve this, for every $(s_3, s_4)$ pair, a set of intermediate signals are computed:

$$\begin{aligned} z_{i1} &= y_{i1} - b(h_{i1}s_3 + h_{i2}s_4), \\ z_{i2} &= y_{i2} - d(h_{i2}s_3^* - h_{i1}s_4^*), \end{aligned} \tag{3.29}$$

which are equal to:

$$\begin{aligned} z_{i1} &= a(h_{i1}s_1 + h_{i2}s_2) + n_{i1}, \\ z_{i2} &= c(h_{i2}s_1^* - h_{i1}s_2^*) + n_{i2}. \end{aligned} \tag{3.30}$$

It can be seen that the expressions in (3.30) may be combined to yield individual estimates for the symbols $s_1$ and $s_2$.

$$\begin{aligned}
\hat{s}_1 &= (h_{11}z_{11} + h_{21}^* z_{21})/a + (h_{12}z_{12}^* + h_{22}z_{22}^*)/c^*, \\
\hat{s}_1 &= (|h_{11}|^2 + |h_{12}|^2 + |h_{21}|^2 + |h_{22}|^2)s_1 + v_1, \\
\hat{s}_2 &= (h_{12}^* z_{11} + h_{22}^* z_{21})/a - (h_{11}z_{12}^* + h_{21}z_{22}^*)/c^*, \\
\hat{s}_2 &= (|h_{11}|^2 + |h_{12}|^2 + |h_{21}|^2 + |h_{22}|^2)s_2 + v_2.
\end{aligned} \tag{3.31}$$

where $v_1$ and $v_2$ are the resultant noise terms after the linear combinations.

Therefore for every $|\mathcal{M}|^2$ $(s_3, s_4)$ pair, we can compute the corresponding ML estimates $(\hat{s}_1^{ML}, \hat{s}_2^{ML})$ of $s_1$ and $s_2$ separately by first normalizing $\hat{s}_1, \hat{s}_2$ (i.e., dividing them by $(|h_{11}|^2 + |h_{12}|^2 + |h_{21}|^2 + |h_{22}|^2)$) and then passing these normalized estimates through a threshold detector. This way instead of computing $|\mathcal{M}|^4$ distance metrics, we may compute $|\mathcal{M}|^2$ possible distance metrics for each $(\hat{s}_1^{ML}, \hat{s}_2^{ML}, s_3, s_4)$. After computing this distance metric shown in (3.32), the quadruplet which minimizes (3.32) will be chosen. This way the receiver complexity is reduced to $|\mathcal{M}|^2$ from $|\mathcal{M}|^4$.

$$\begin{aligned}
D(s_1, s_2, s_3, s_4) = \{&|y_{11} - h_{11}(as_1 + bs_4) - h_{12}(as_2 + bs_4)|^2 \\
&+ |y_{12} - h_{11}(-cs_2^* - ds_4^*) - h_{12}(as_1^* + ds_3^*)|^2 \\
&+ |y_{21} - h_{21}(as_1 + bs_4) - h_{22}(as_2 + bs_4)|^2 \\
&+ |y_{22} - h_{21}(-cs_2^* - ds_4^*) - h_{12}(as_1^* + ds_3^*)|^2\}.
\end{aligned} \tag{3.32}$$

It must be noted that the detection scheme outlined above is optimal when $|a| = |c|$, or $|b| = |d|$ if detection is carried out for a given $(s_1, s_2)$ pair. Furthermore, the design parameters $a, b, c, d$ given in (3.27) should be optimized to achieve full diversity and high coding gain. However they are restricted with the following transmit power constraints

$$\begin{aligned}
|a|^2 + |b|^2 = |c|^2 + |d|^2 = 1, \\
|a|^2 + |c|^2 = |b|^2 + |d|^2 = 1,
\end{aligned} \tag{3.33}$$

where the first equality guarantees equal transmit power at each time instant and the second guarantees equal transmit power for each symbol. These equalities may be combined with the optimal detection constraint $|a| = |c|$ and $|b| = |d|$, which yields

$$|a|^2 = |b|^2 = |c|^2 = |d|^2 = 1/\sqrt{2}. \tag{3.34}$$

### 3.4.3 Reduced Complexity TAST SF Code

Making use of the algorithm presented in the previous section, we may combine the elements of (3.24) to obtain a code structure similar to (3.27) which will allow for the detection complexity to be reduced. The resulting code matrix, again shown only for the first 4 subcarriers is

$$\begin{bmatrix} ax_{11}+b(\phi^{1/4}x_{21}) & -cx_{12}^*-d(\phi^{1/4}x_{22})^* & 0 & 0 \\ ax_{12}+b(\phi^{1/4}x_{22}) & cx_{11}^*+d(\phi^{1/4}x_{21})^* & 0 & 0 \\ 0 & 0 & ax_{13}+b(\phi^{1/4}x_{23}) & -cx_{14}^*-d(\phi^{1/4}x_{24})^* \\ 0 & 0 & ax_{14}+b(\phi^{1/4}x_{24}) & cx_{13}^*+d(\phi^{1/4}x_{23})^* \end{bmatrix}. \\ \rightarrow Subcarrier \tag{3.35}$$

Recall that the decoding complexity for (3.24) was $|\mathcal{M}|^8$. We will show how to make this complexity as low as $|\mathcal{M}|^4$. To illustrate the detection scheme, first the received signals are written as

$$\begin{aligned} y_{i,1} &= \tilde{H}_{i1}(1)\left(ax_{11}+b\phi^{1/4}x_{21}\right)+\tilde{H}_{i2}(1)\left(ax_{12}+b\phi^{1/4}x_{22}\right)+v_i(1), \\ y_{i,2} &= \tilde{H}_{i1}(2)\left(-cx_{12}^*-d(\phi^{1/4}x_{22})^*\right)+\tilde{H}_{i2}(2)\left(cx_{11}^*+d(\phi^{1/4}x_{21})^*\right)+v_i(2), \\ y_{i,3} &= \tilde{H}_{i3}(3)\left(ax_{13}+b(\phi^{1/4}x_{23})\right)+\tilde{H}_{i4}(3)\left(ax_{14}+b(\phi^{1/4}x_{24})\right)+v_i(3), \\ y_{i,4} &= \tilde{H}_{i3}(4)\left(-cx_{14}^*-d(\phi^{1/4}x_{24})^*\right)+\tilde{H}_{i4}(4)\left(cx_{13}^*+d(\phi^{1/4}x_{23})^*\right)+v_i(4). \end{aligned} \tag{3.36}$$

where $y_{i,k}$ represents the received signal at receive antenna $i$ at subcarrier index $k$ and $v_i(k)$ is the i.i.d noise with variance $N_0/2$ per dimension. $\tilde{H}_{ij}(k)$ is the frequency response of the channel from transmit antenna $j$ to receive antenna $i$ at subcarrier index $k$ as described in Section 3.2. For simplicity the detection scheme analyzed here is only for the first 4 subcarriers since the remainder of the subcarriers follow the same principle. It must be noted that the parameters $a, b, c, d$ must also follow the constraints given in (3.34).

For a given $(s_{21}, s_{22}, s_{23}, s_{24})$ quadruplet, $(x_{21}, x_{22}, x_{23}, x_{24})^T = \mathbf{M}\,(s_{21}, s_{22}, s_{23}, s_{24})^T$ is computed. We will use $(s_{21}, s_{22}, s_{23}, s_{24})$ and $(x_{21}, x_{22}, x_{23}, x_{24})$ interchangeably since the mapping is unique. Therefore the intermediate signals for a given

quadruplet $(x_{21}, x_{22}, x_{23}, x_{24})$ can be written as

$$\begin{aligned}
z_{i,1} &= y_{i,1} - b\left(\tilde{H}_{i1}(1)\phi^{1/4}x_{21} + \tilde{H}_{i2}(1)\phi^{1/4}x_{22}\right), \\
z_{i,2} &= y_{i,2} - d\left(\tilde{H}_{i2}(2)(\phi^{1/4}x_{21})^* - \tilde{H}_{i1}(2)(\phi^{1/4}x_{22})^*\right), \\
z_{i,3} &= y_{i,3} - b\left(\tilde{H}_{i3}(3)\phi^{1/4}x_{23} + \tilde{H}_{i4}(3)\phi^{1/4}x_{24}\right), \\
z_{i,4} &= y_{i,4} - d\left(\tilde{H}_{i4}(4)(\phi^{1/4}x_{23})^* - \tilde{H}_{i3}(4)(\phi^{1/4}x_{24})^*\right),
\end{aligned} \tag{3.37}$$

which are equal to

$$\begin{aligned}
z_{i,1} &= a\left(\tilde{H}_{i1}(1)x_{11} + \tilde{H}_{i2}(1)x_{12}\right) + v_i(1), \\
z_{i,2} &= c\left(\tilde{H}_{i2}(2)x_{11}^* - \tilde{H}_{i1}(2)x_{12}^*\right) + v_i(2), \\
z_{i,3} &= a\left(\tilde{H}_{i3}(3)x_{13} + \tilde{H}_{i4}(3)x_{14}\right) + v_i(3), \\
z_{i,4} &= c\left(\tilde{H}_{i4}(4)x_{13}^* - \tilde{H}_{i3}(4)x_{14}^*\right) + v_i(4).
\end{aligned} \tag{3.38}$$

The estimates for $x_{11}$ and $x_{12}$ may be computed using (3.39) and (3.40) may be used to compute the estimates for $x_{13}$ and $x_{14}$ as follows;

$$\begin{aligned}
\hat{x}_{11} &= \sum_{i=1}^{4} \tilde{H}_{i1}^*(2)z_{i,1}/a + \sum_{i=1}^{4} \tilde{H}_{i2}(1)z_{i,2}^*/c^*, \\
&= \left(\sum_{i=1}^{4} \tilde{H}_{i1}^*(2)\tilde{H}_{i1}(1) + \sum_{i=1}^{4} \tilde{H}_{i2}(1)\tilde{H}_{i2}^*(2)\right) x_{11} + \tilde{v}_1, \\
\hat{x}_{12} &= \sum_{i=1}^{4} \tilde{H}_{i2}^*(2)z_{i,1}/a - \sum_{i=1}^{4} \tilde{H}_{i1}(1)z_{i,2}^*/c^*, \\
&= \left(\sum_{i=1}^{4} \tilde{H}_{i2}^*(2)\tilde{H}_{i2}(1) + \sum_{i=1}^{4} \tilde{H}_{i1}(1)\tilde{H}_{i1}^*(2)\right) x_{12} + \tilde{v}_2,
\end{aligned} \tag{3.39}$$

$$\begin{aligned}
\hat{x}_{13} &= \sum_{i=1}^{4} \tilde{H}_{i3}^*(4)z_{i,3}/a + \sum_{i=1}^{4} \tilde{H}_{i4}(3)z_{i,4}^*/c^*, \\
&= \left(\sum_{i=1}^{4} \tilde{H}_{i3}^*(4)\tilde{H}_{i3}(3) + \sum_{i=1}^{4} \tilde{H}_{i4}(3)\tilde{H}_{i4}^*(4)\right) x_{13} + \tilde{v}_3, \\
\hat{x}_{14} &= \sum_{i=1}^{4} \tilde{H}_{i4}^*(4)z_{i,3}/a - \sum_{i=1}^{4} \tilde{H}_{i3}(3)z_{i,4}^*/c^*, \\
&= \left(\sum_{i=1}^{4} \tilde{H}_{i4}^*(4)\tilde{H}_{i4}(3) + \sum_{i=1}^{4} \tilde{H}_{i3}(3)\tilde{H}_{i3}^*(4)\right) x_{14} + \tilde{v}_4.
\end{aligned} \tag{3.40}$$

We can normalize these estimates by dividing $\hat{x}_{mn}$ by the coefficient of $x_{mn}$. For example, the normalized estimate $\tilde{x}_{11}$ can be computed as

$$\tilde{x}_{11} = \hat{x}_{11} \Bigg/ \left( \sum_{i=1}^{4} \tilde{H}_{i1}^{*}(2)\tilde{H}_{i1}(1) + \sum_{i=1}^{4} \tilde{H}_{i2}(1)\tilde{H}_{i2}^{*}(2) \right), \tag{3.41}$$

and the remainder of the normalized estimates $\tilde{x}_{12}, \tilde{x}_{13}, \tilde{x}_{14}$ may be computed in a similar fashion from (3.39) and (3.40). Note that we assume $H_{ij}(1) = H_{ij}(2)$ for optimal detection. We can put the normalized estimates in

$$\text{inv}(\mathbf{M})(\tilde{x}_{11}, \tilde{x}_{12}, \tilde{x}_{13}, \tilde{x}_{14})^T = (\hat{s}_{11}, \hat{s}_{12}, \hat{s}_{13}, \hat{s}_{14})^T, \tag{3.42}$$

since originally the data symbols underwent the complex rotation $(x_{11}, x_{12}, x_{13}, x_{14})^T = \mathbf{M}\,(s_{11}, s_{12}, s_{13}, s_{14})^T$. After this we can send the estimated data symbols $(\hat{s}_{11}, \hat{s}_{12}, \hat{s}_{13}, \hat{s}_{14})$ through a threshold detector and decide on the data symbols which were sent for a given quadruplet $(s_{21}, s_{22}, s_{23}, s_{24})$. Let us assume that for the input $(\hat{s}_{11}, \hat{s}_{12}, \hat{s}_{13}, \hat{s}_{14})$, the output of the threshold detector is $(\bar{s}_{11}, \bar{s}_{12}, \bar{s}_{13}, \bar{s}_{14})$. The next step is to compute the Euclidean distance associated with this estimate. For this step the complex rotation matrix will once again be used but this time on the data vector $(\bar{s}_{11}, \bar{s}_{12}, \bar{s}_{13}, \bar{s}_{14})$, such that given the quadruplet $(x_{21}, x_{22}, x_{23}, x_{24})$, the final estimates for $(x_{11}, x_{12}, x_{13}, x_{14})$ are

$$(\bar{x}_{11}, \bar{x}_{12}, \bar{x}_{13}, \bar{x}_{14})^T = \mathbf{M}\,(\bar{s}_{11}, \bar{s}_{12}, \bar{s}_{13}, \bar{s}_{14})^T\,. \tag{3.43}$$

The Euclidean distance is computed as follows

$$\begin{aligned} D(\bar{x}_{11}, \bar{x}_{12}, \bar{x}_{13}, \bar{x}_{14}, x_{21}, x_{22}, x_{23}, x_{24}) = \\ \sum_{i=1}^{4} \left| y_{i,1} - \tilde{H}_{i1}(1)\left(a x_{11} + b\phi^{1/4} x_{21}\right) + \tilde{H}_{i2}(1)\left(a\bar{x}_{12} + b\phi^{1/4} x_{22}\right) \right|^2 \\ + \sum_{i=1}^{4} \left| y_{i,2} - \tilde{H}_{i1}(2)\left(-c x_{12}^{*} - d(\phi^{1/4} x_{22})^{*}\right) + \tilde{H}_{i2}(2)\left(c\bar{x}_{11}^{*} + d(\phi^{1/4} x_{21})^{*}\right) \right|^2 \\ + \sum_{i=1}^{4} \left| y_{i,3} - \tilde{H}_{i3}(3)\left(a\bar{x}_{13} + b(\phi^{1/4} x_{23})\right) + \tilde{H}_{i4}(3)\left(a\bar{x}_{14} + b(\phi^{1/4} x_{24})\right) \right|^2 \\ + \sum_{i=1}^{4} \left| y_{i,4} - \tilde{H}_{i3}(4)\left(-c\bar{x}_{14}^{*} - d(\phi^{1/4} x_{24})^{*}\right) + \tilde{H}_{i4}(4)\left(c\bar{x}_{13}^{*} + d(\phi^{1/4} x_{23})^{*}\right) \right|^2. \end{aligned} \tag{3.44}$$

A total of $|\mathcal{M}|^4$ Euclidean distances will be computed and the input vector $(\bar{x}_{11}, \bar{x}_{12}, \bar{x}_{13}, \bar{x}_{14}, x_{21}, x_{22}, x_{23}, x_{24})$ minimizing (3.44) will be selected. The decided rotated symbol vector will then be converted to the data symbols $s_{mn}$ by using the inverse operation of (3.25).

## 3.5 Simulation Results

The aim of this section is to evaluate the performance of the techniques mentioned in Sections 3.3 and 3.4. We have used Matlab to simulate the physical layer and to study bit error rate (BER) and block error rate (BLER) performance under different channel conditions and varying system parameters such as coding schemes.

For the sake of simplicity we have made some general assumptions. First of all, the antenna separation in the transmit and receive antenna arrays is assumed to be sufficient such that there is independent fading between each transmit and receive antenna pair. Furthermore, perfect frequency synchronization and CSI are assumed to be present at the receiver.

The system parameters used in the simulations are based on the evaluation methodology document (EMD) [42] and the IEEE 802.16e standard and are summarized in Table 3.1. The modulation type is chosen depending on the MIMO technique such that the resulting spectral efficiency is equal to 4 bits/sec/Hz. For codes with rate equal to 2 symbols/pcu we choose QPSK and for codes with rate equal to 1 symbol/pcu we choose 16-QAM. The power delay profiles of the modified ITU channels are given in Table 3.2.

We analyze the performance of various MIMO techniques in terms of BER. When channel coding is implemented, an additional performance metric is the BLER. The performance curves are plotted against $E_b/N_0$ per receive antenna, i.e., SNR per transmitted bit per receive antenna, where $E_b$ is energy per transmitted bit and $N_0/2$ represents the noise variance per dimension. The energy per transmitted bit, $E_b$, can be expressed as

$$E_s = E_b \times \log_2(\mathcal{M}), \tag{3.45}$$

where $E_s$ is the average energy per symbol belonging to the $\mathcal{M}$-ary signal constellation which is always normalized such that $E_s = 1$.

Table 3.1: Simulation parameters

| | |
|---|---|
| MIMO configuration ($M_T \times M_R$) | 2×2, 4×4 |
| Carrier frequency ($f_c$) | 2.5 GHz |
| Total bandwidth | 10 MHz |
| FFT size ($N$) | 1024 |
| Sampling frequency | 11.2 MHz |
| Subcarrier spacing | 10.9375 KHz |
| Cyclic prefix length (fraction of FFT size) | 1/8 |
| OFDMA symbol duration with cyclic prefix | 102.86 $\mu$s (for CP=1/8) |
| FEC type | Convolutional Coding (CC)<br>Convolutional Turbo Coding (CTC) |
| FEC block size | 96 or 480 bits |
| FEC rate | 1/2 |
| Channel model | Modified ITU-Ped B, ITU-VehA [42] |
| Mobile speeds | 3 km/hr (Modified ITU-Ped B)<br>30 km/hr (Modified ITU-Veh A )<br>120 km/hr (Modified ITU-Veh A ) |
| Modulation type | QPSK or 16-QAM |
| Subchannelization schemes | Band AMC<br>PUSC |

Table 3.2: Modified ITU channels

| **Modified ITU-Ped B** | | **Modified ITU-Veh A** | |
|---|---|---|---|
| Power (dB) | Delay (ns) | Power (dB) | Delay (ns) |
| -1.175 | 0 | -3.1031 | 0 |
| 0 | 40 | -0.4166 | 50 |
| -0.1729 | 70 | 0 | 90 |
| -0.2113 | 120 | -1.0065 | 130 |
| -0.2661 | 210 | -1.4083 | 270 |
| -0.3963 | 250 | -1.4436 | 300 |
| -4.32 | 290 | -1.5443 | 390 |
| -1.1608 | 350 | -4.0437 | 420 |
| -10.4232 | 780 | -16.6369 | 670 |
| -5.7198 | 830 | -14.3955 | 750 |
| -3.4798 | 880 | -4.9259 | 770 |
| -4.1745 | 920 | -16.516 | 800 |
| -10.1101 | 1200 | -9.2222 | 1040 |
| -5.646 | 1250 | -11.9058 | 1060 |
| -10.0817 | 1310 | -10.1378 | 1070 |
| -9.4109 | 1350 | -14.1861 | 1190 |
| -13.9434 | 2290 | -16.9901 | 1670 |
| -9.1845 | 2350 | -13.2515 | 1710 |
| -5.5766 | 2380 | -14.8881 | 1820 |
| -7.6455 | 2400 | -30.348 | 1840 |
| -38.1923 | 3700 | -19.5257 | 2480 |
| -22.3097 | 3730 | -19.0286 | 2500 |
| -26.0472 | 3760 | -38.1504 | 2540 |
| -21.6155 | 3870 | -20.7436 | 2620 |

### 3.5.1 Performance without FEC

We begin by analyzing the performance when there is no FEC block before the ST modulation block. Although there is no WiMAX profile in which FEC is not present, it is still useful to analyze the performance so that the gains obtained via FEC may be better visualized. The subchannelization scheme is chosen as band AMC and all the available subcarriers are allocated to a single user such that error performance may be analyzed independent of any scheduling and resource allocation method.

The performance of various techniques without FEC for various user mobilities is presented in Figures 3.4 to 3.6. As mentioned earlier, ST-Alamouti and the Golden Code relies on the channel response to remain constant for two symbol periods, therefore channel gain variations between successive OFDM symbols can degrade performance. When mobility is added to the system such that the channel becomes a time-varying channel, the assumption that the channel stays constant over 2 symbol intervals is no longer valid, so in order to keep the decoding complexity linear, decisions are made based on constant channel assumption.

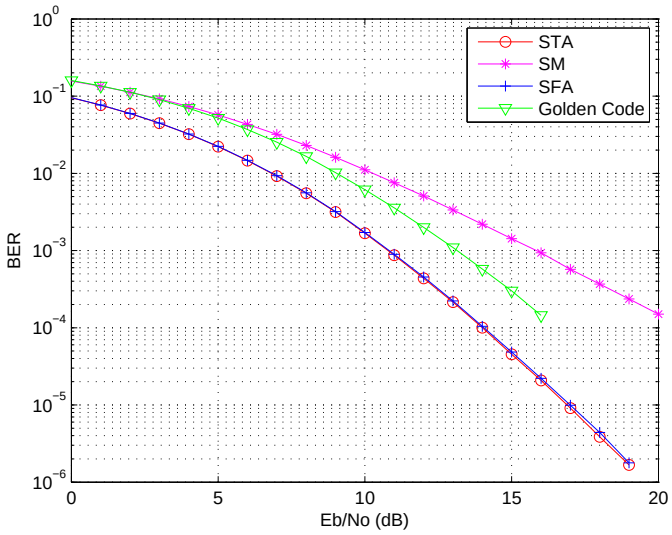


Figure 3.4: Performance of the system without FEC under v=3 km/hr.

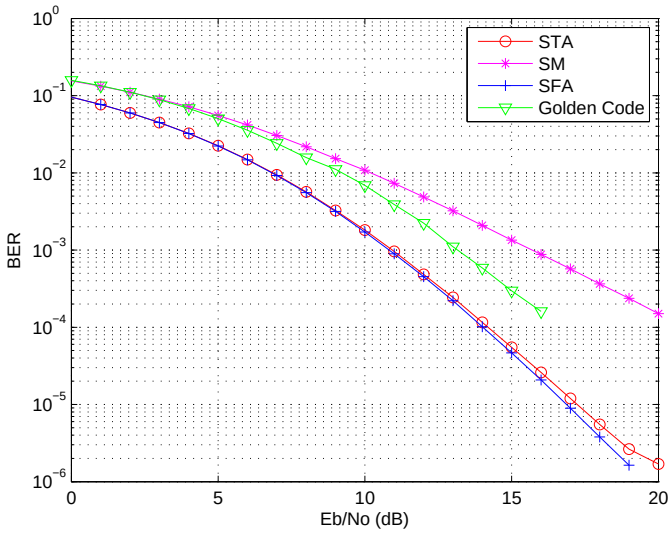


Figure 3.5: Performance of the system without FEC under v=30 km/hr.

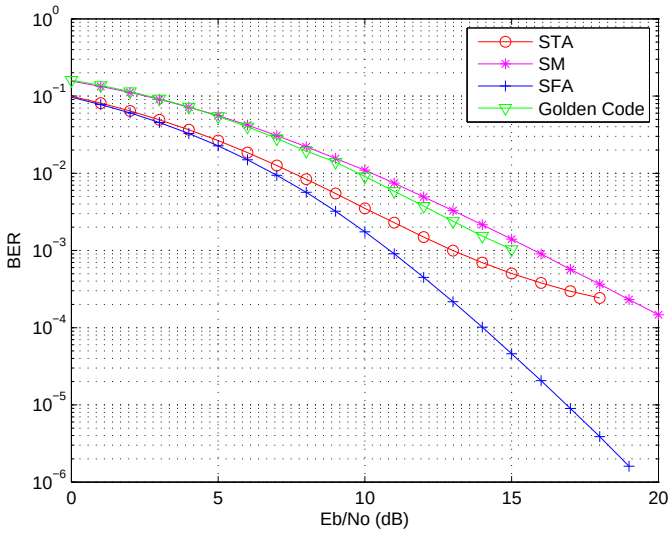


Figure 3.6: Performance of the system without FEC under v=120 km/hr.

With SF-Alamouti, decisions can be made in one OFDM symbol so it is expected that SF-Alamouti performs better in fast fading environments. However in this case, adjacent subcarriers should have identical gains for optimal linear decoding. A suboptimal but linear decoding is based on constant channel assumption but variations between adjacent subcarriers due to the frequency selective nature of the channel will introduce errors in the decoding process and possibly degrade performance. However, as pointed out in Section 3.4, because

we have a large FFT size the variations are minimal and there is a small performance loss.

Furthermore, in the presence of mobility and at higher SNR, the curves start to exhibit an error floor, which is a well known characteristic of OFDM systems in Doppler channels [43]. As mobility increases the channel gains start to change much more rapidly and ST-Alamouti and Golden code performance is degraded. SM and SF-Alamouti is much more robust against mobility and may allow the use of slightly higher order of modulation/coding. It can be seen that SF-Alamouti has nearly the same performance for all speeds while ST-Alamouti and Golden Code performance deteriorates.

### 3.5.2 Performance with FEC

The variation in the performance of the system when used with a channel coding technique such as CC or CTC is presented next. The CC given in Section 8.4.9.2.1 and the CTC given in Section 8.4.9.2.3 of the IEEE 802.16e standard [44] are considered. Again the subchannelization scheme is chosen as band AMC and all the available subcarriers are allocated to a single user.

The first channel coding technique we investigate is the convolutional code. We implement the tail-biting CC with rate 1/2, constraint length equal to $K = 7$ and generator polynomials

$$G_1 = [171]_{OCT},$$
$$G_2 = [133]_{OCT}.$$

When CTC is used the interleaver block is not implemented, since a subblock interleaver is used within the CTC encoder. It should be noted that in both the CC and CTC cases the interleaving process provides additional frequency diversity since FEC coded bits which are originally adjacent to each other are mapped onto nonadjacent subcarriers.

The effects of FEC can be seen in Figure 3.7 for ST-Alamouti and SM with FEC block size equal to 96 bits. It can be seen that a coding gain of approximately 9 dB may be achieved in both cases. The coded systems also exhibit the irreducible error floor which can be seen clearly for the case of ST-Alamouti at $v = 120$ km/hr.

The performance of SM and ST Alamouti are compared under different vehicular speeds. SM also makes decisions in one OFDM symbol therefore is not affected by the mobility in the channel. However, since spatial multiplexing does not make use of any kind of diversity, its performance is much worse than ST-Alamouti. The performance of coded SM approaches the uncoded ST-Alamouti curves at very low mobility. It can be said that even though FEC provides protection from errors; the numerical results demonstrate that transmit diversity is indispensable for better performance.

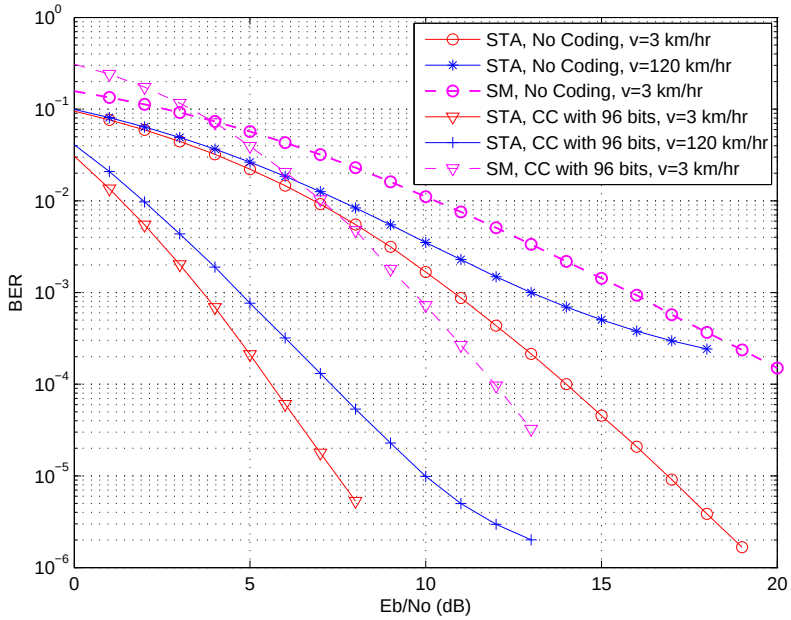


Figure 3.7: Effects of channel coding on performance.

We have also compared the effect FEC block size has on error performance. When FEC size increases from 96 bits 480 bits there is an improvement in performance as can be seen in Figure 3.8. It can be seen that up to 3 dB gain may be achieved when block size is increased form 96 bits to 480 bits. Therefore from this point onwards we will take the FEC block size as 480 bits due to its superior performance.

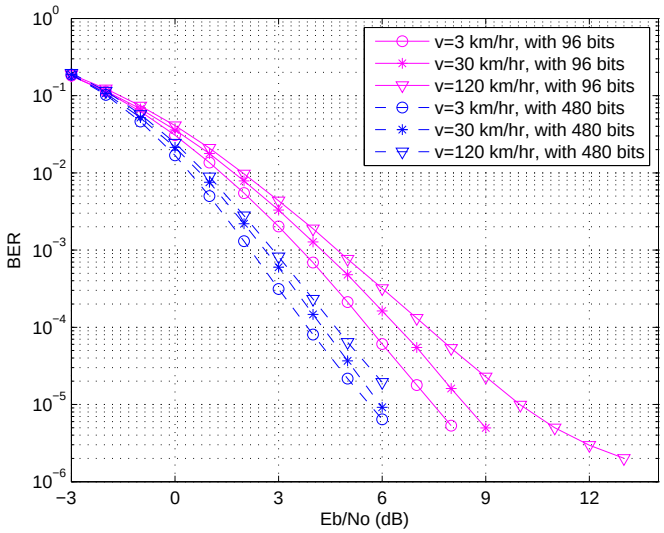


(a) ST-Alamouti performance.

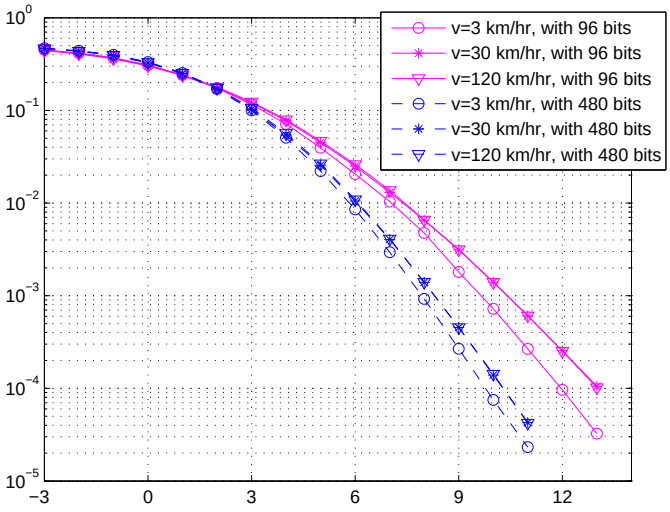


(b) SM performance.

Figure 3.8: The effect of increasing FEC block size on ST-Alamouti and SM.

Furthermore, for ST-Alamouti we also demonstrate the performance of different FEC block sizes for user speed equal to $v = 3$ km/hr in Figure 3.9. It can be seen here that at higher FEC block sizes the effect of increased block size on performance diminishes. This is because due to the interleaving process when a higher block size is used, bits are scattered across a larger frequency band therefore creating higher frequency diversity. If the subchannelization scheme is changed to PUSC, the effect of block size on performance becomes very small since PUSC provides significant frequency diversity.

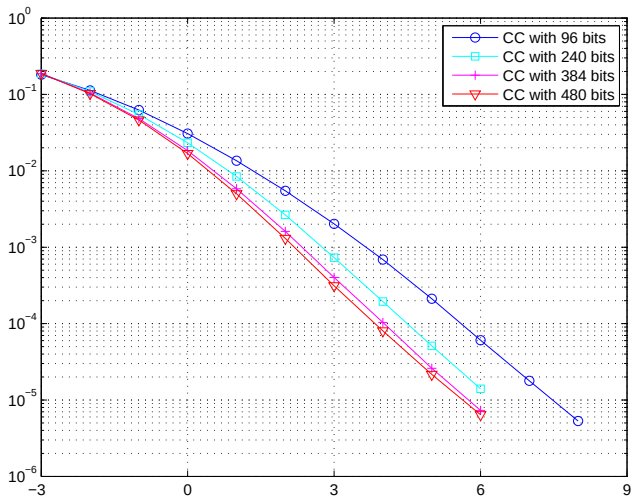


(a) ST-Alamouti performance with band AMC.

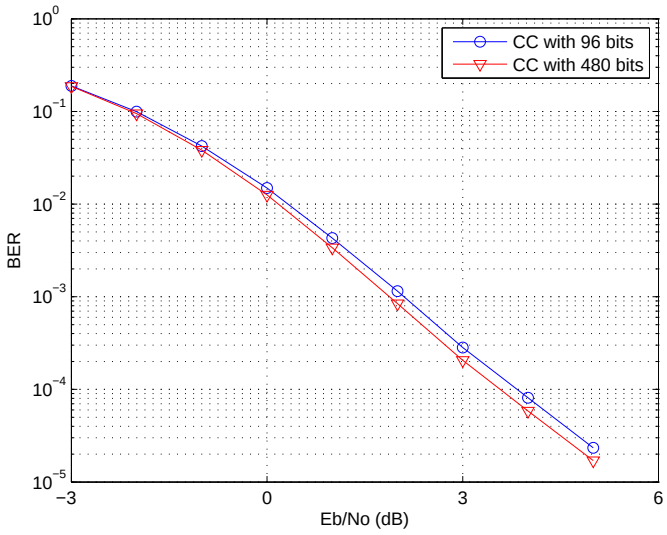


(b) ST-Alamouti performance with PUSC.

Figure 3.9: The effect of increasing FEC block size on ST-Alamouti for different subchannelization schemes.

We now consider the CTC with rate 1/2 as the FEC code using band AMC and evaluate the performance benefits. In Figure 3.10, we compare the performance of ST-Alamouti and SM using CTC and CC with a block size of 480 bits. It can be seen that CTC provides an additional 1.5 dB gain for ST-Alamouti and 2 dB gain for SM in comparison to CC. Therefore we will consider CTC instead of CC as the coding scheme from this point on since it provides better error performance.

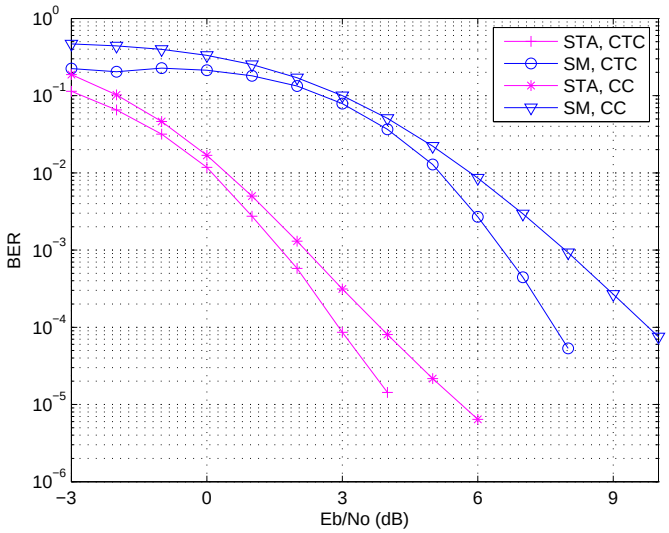


Figure 3.10: Performance comparison of CTC and CC under v=3 km/hr.

The performance of CTC under different user mobilities and MIMO techniques is presented next in Figure 3.11. The presented TAST code is the reduced complexity code given in (3.33). It can be seen that the TAST code outperforms other codes and is more immune to mobility. It should be noted that the performance of the TAST code is for a $4 \times 4$ system and is given here to demonstrate that its performance is nearly unaffected by the mobility in the channel.

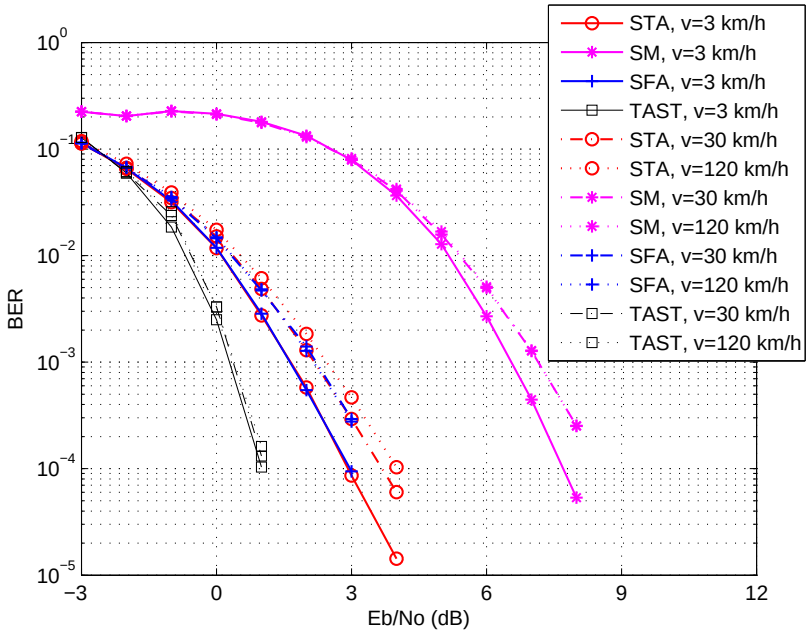


Figure 3.11: Performance comparison of different MIMO techniques with CTC under various user speeds.

For the reduced complexity TAST code presented above we have chosen the parameters $a, b, c, d$ the same as those given in [9], i.e.,

$$a = c = \frac{1}{\sqrt{2}}, \quad b = \frac{(1-\sqrt{7}) + j(1+\sqrt{7})}{4\sqrt{2}}, \quad d = -jb. \tag{3.46}$$

However, it should be noted that the choice of the variables $a, b, c, d$ greatly affect the performance through the coding gain of the code. Therefore, we have performed particle swarm optimization method to optimize the coding gain such that a better performance may be achieved. However after many experiments, we were able to improve it only slightly. The new parameters are

$$\begin{aligned} a &= -0.7056 - 0.0457j, \ b = 0.1684 + 0.6868j \\ c &= 0.2333 + 0.6675j, \ d = 0.6667 + 0.2356j. \end{aligned} \tag{3.47}$$

The improvement is shown in Figure 3.12 along with the higher complexity TAST code given in (3.24).

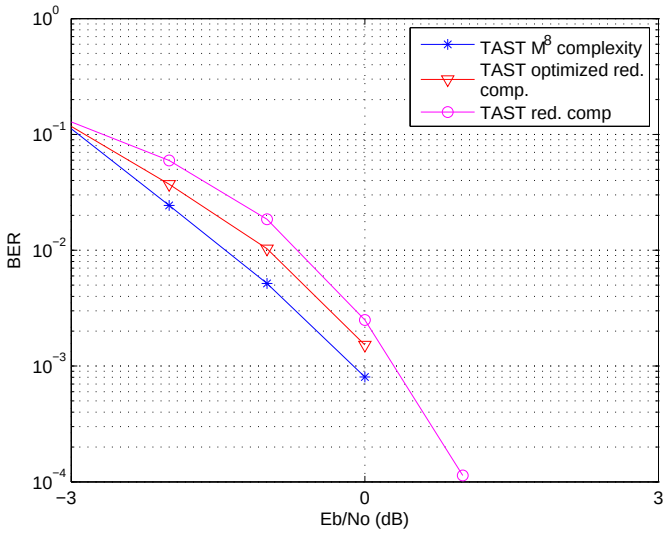


Figure 3.12: Performance comparison of TAST code for different decoding complexities, v=3 km/hr.

We also compare the performance of the TAST code with Matrix A and B given in (3.13) and (3.14) in Figure 3.13 in a $4 \times 4$ system. It can be seen that Matrix A has superior performance, while Matrix B exhibits a worse performance than the TAST code. Recall that in Matrix B 2 Alamouti schemes

were multiplexed over 4 antennas which the results in interference between the 2 Alamouti blocks. Matrix B has a rate of 2 symbols/pcu (similar to the TAST code) and therefore we have used QPSK. Since Matrix A does not suffer from this interference, ever with a higher constellation size (16-QAM) it still has a better performance.

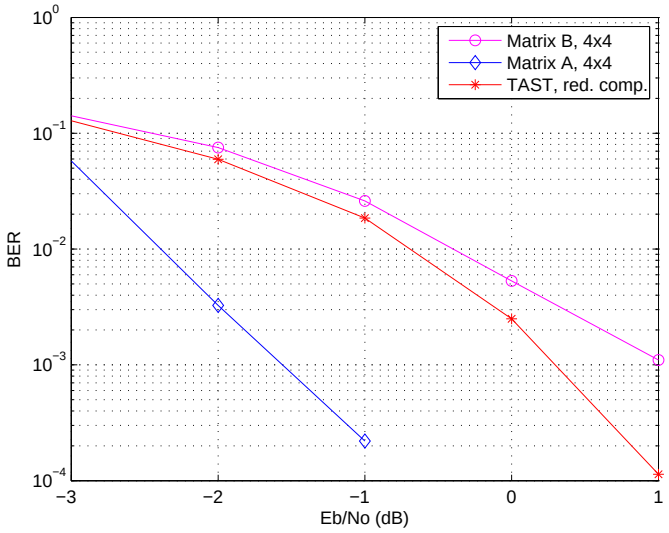


Figure 3.13: Performance comparison of TAST code and Matrix A and B, v=3 km/hr.

Another appropriate performance metric for comparison might be the block error rate (BLER), based the error of FEC blocks. In Figure 3.14 , BLER of ST/SF Alamouti, SM and the TAST code are compared. To reach a BLER of $10^{-2}$, ST and SF Alamouti require approximately 1.7 dB, SM requires nearly 6.7 dB and the TAST code requires 0.3 dB as shown in the Figure 3.14.

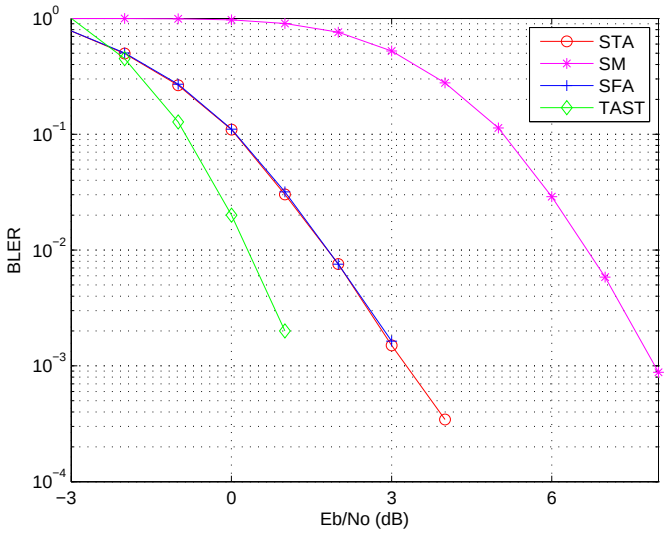


Figure 3.14: Block error rate performance comparison.

The physical layer also allows for different subchannelization schemes. Subchannels can be constructed using either contiguous subcarriers or subcarriers pseudorandomly distributed across the frequency spectrum. Up to this point, the presented results used band-AMC, i.e., contiguous mapping of data subcarriers to subchannels. PUSC is another subchannelization scheme based on distributed carriers for both the uplink and the downlink in WiMAX. In PUSC subchannels are formed using subcarriers distributed over the whole frequency band and therefore they provide more frequency diversity [45].

This additional frequency diversity is especially beneficial for ST-Alamouti which doesn't provide any frequency diversity if not implemented in conjunction with PUSC. However PUSC is disadvantageous in the case of SF codes (SFC), such as SF-Alamouti. As mentioned earlier, in SFC, adjacent subcarriers should have identical gains for optimal linear complexity decoding which is a valid when band AMC is used as the subchannelization scheme. However when SFC is used in conjunction with PUSC the adjacent data symbols are mapped to subcarriers which are far away from each other and therefore experience vastly different channels. Because of the difference in channel conditions the signals at the linear receiver do not coherently combine which in turn leads to significant SNR and performance losses.

The performance comparison of various codes with PUSC and band AMC is shown in Figure 3.15. It can be seen that the performance of ST-Alamouti and

SM improves due to PUSC while SF-Alamouti performance degrades. Therefore ST-Alamouti should be used instead of SF-Alamouti since the performance loss is significant in SF-Alamouti case due to PUSC.

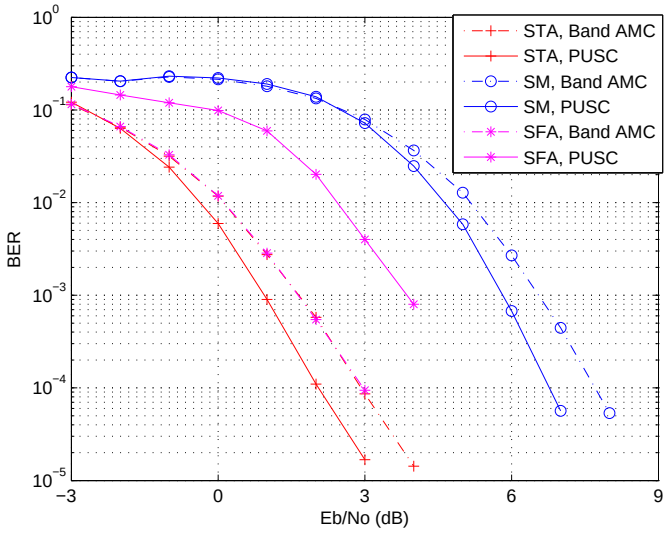


Figure 3.15: Performance comparison of PUSC and band AMC.

### 3.5.3 Performance with Intercarrier Interference

Another important consideration is the effects of intercarrier interference (ICI) on the performance since it is well known that in multicarrier systems performance losses occur due to ICI. ICI may be caused by imperfect frequency synchronization and in high mobility scenarios when the Doppler spread is large. For our work we assume that there exists perfect frequency synchronization and only analyze the effects of ICI caused by the mobility present in the channel. For low mobility cases when the channel is slow fading such that it remains constant during an OFDM symbol, ICI can be assumed to be insignificant.

When there is high mobility in the system such that the channel becomes highly time variant, the variations disrupt the orthogonality of the subcarriers and cause ICI. In those cases, a more complex system is needed to model such behavior. To study the effect of ICI on the performance of the proposed SF code, we make use of the analysis provided in [46]. In this analysis, for any given subcarrier the data on other subcarriers causing ICI are multiplied by a channel dependant function and become additive terms just like the noise term. The magnitude of the additive term depends on how fast the channel is changing.

The time varying channel is obtained by sampling it at 11.2 MHz which is the sampling frequency of the OFDM symbol as given in Table 3.1.

We may modify the received signal given in (3.5) to incorporate the ICI term derived in [46]. We omit the OFDM symbol index $u$ for simplicity. The received signal at receive antenna $i$ at subcarrier $k$ may be expressed as

$$y_i(k) = \frac{1}{\sqrt{M_T}} \sum_{j=1}^{M_T} \left( G_{ij}(k,k)s_j(k) + \underbrace{\sum_{q=0, q\neq k}^{N-1} G_{ij}(k,q)s_j(q)}_{ICI(k)} \right) + v_i(k), \quad (3.48)$$

where

$$G_{ij}(m,n) = \frac{1}{N} \sum_{r=0}^{N-1} \sum_{l=0}^{L-1} \alpha_{ij}(l,r) e^{j2\pi r(n-m)/N} e^{-j2\pi nl/N}. \quad (3.49)$$

The channel dependant function $G_{ij}$ is obtained by the time-variant path gain $\alpha_{ij}(l,r)$, where $l$ indicates the tap index and $r$ indicates the time index. It can be seen that the second term inside the summation in (3.48) is the additional ICI term caused by the data on all the other subcarriers.

The performance of the proposed TAST code and ST-Alamouti is analyzed with and without ICI in Figures 3.16 and 3.17. For these simulations user mobility is taken as 120 km/hr, since this is a high mobility case. For the no ICI case, the simulations are carried assuming that the channel stays constant during an OFDM symbol and the effects of ICI are ignored. For the ICI case, we take into account the variations in the channel during an OFDM symbol therefore this is a more realistic performance metric. The receiver structure assumed is based on no ICI assumption such that the ICI term is treated as additional noise. Fortunately, it can be seen that there is at most 0.5 dB performance loss at $v = 120$ km/hr when we take ICI into account. However it is clear that the performance gap will increase as SNR increases. The performance loss is not very large because even with a user speed of 120 km/hr, the coherence time is found to be approximately 1.52 ms, which is a duration approximately 14 OFDM symbols long. The coherence time, $T_c$, is calculated using the formula $T_c = 0.423/f_d$ [1], where the Doppler spread for a user speed of 120 km/hr at carrier frequency 2.5 GHz is $f_d = 277.7$ Hz.

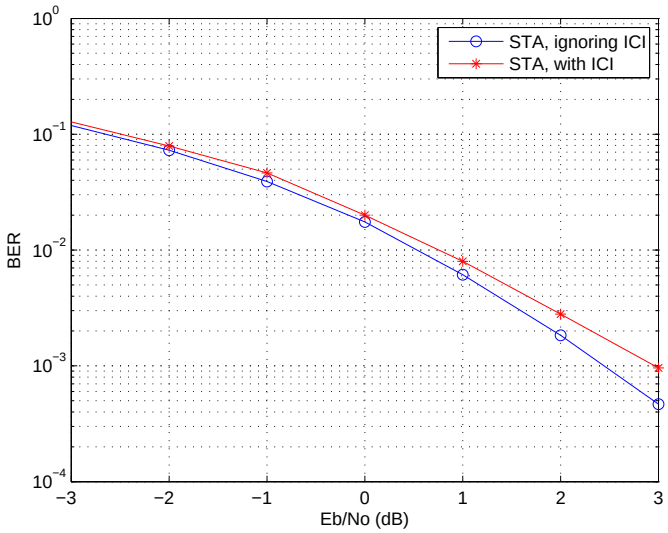


Figure 3.16: Performance comparison with and without ICI for ST-Alamouti.

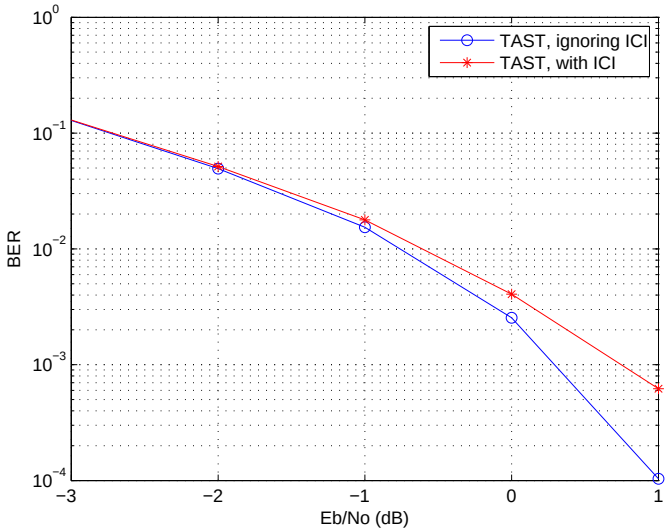


Figure 3.17: Performance comparison with and without ICI for TAST code.

## 3.6 Concluding Remarks

It can be concluded that different channel conditions require the use of different MIMO techniques to meet the performance criteria. When there is high mobility in the system, ST-Alamouti performance with linear receivers deteriorates

because the constant channel assumption of 2 consecutive OFDM symbols does not hold. When there is high mobility in the system SF-Alamouti should be used since it can make decisions in 1 OFDM symbol and therefore is not affected by mobility. The proposed TAST code exhibits a superior performance at the expense of increased decoding complexity which is a fundamental issue that will limit its deployment in practice.

When the subchannelization scheme is band AMC, in SF coding the variation between subcarriers caused by high delay spread was not significant. Therefore, it was more feasible to use SF-Alamouti than ST-Alamouti. However, when PUSC is used, because adjacent subcarriers are distributed across the frequency band, the variation between every pair of subcarriers no longer has negligible effect on performance and therefore SF codes suffer performance losses.

Furthermore, it was shown that both FEC and PUSC add to the frequency diversity of the system. It can be said that at low mobility PUSC and ST-Alamouti should be used for improved performance and at high mobility we may use SF codes with band AMC.

# Chapter 4

# Base Station Cooperation Using Alamouti Space-Time Coding

In this chapter we investigate base station (BS) cooperation in a multicellular network. In multicellular systems, cochannel interference (CC) is typically caused when adjacent cells use the same frequency band. If CC is not mitigated it becomes an important performance degrading factor, especially for users which are near the cell boundaries. A simple way to mitigate CC is to use different frequency bands in adjacent cells such that the interference is minimized. However this in turn decreases the spectral efficiency since in each cell only a fraction of the available frequency band is used. To achieve high spectral efficiencies, such as those required in WiMAX, each cell must make use of the whole available frequency band, i.e., frequency reuse factor must be equal to 1, while mitigating CC using other spectrally more efficient techniques.

BS cooperation is a promising technique to mitigate CC. BSs are already connected to each other with high speed wired links which facilitate information sharing among the BSs and cooperative data transmission. BSs can act as distributive antenna systems to make collaborative MIMO transmissions. However, it should be noted that BS cooperation typically assumes full channel state information (CSI) at the BSs. The CSI may be obtained during the uplink phase and each BS may share the CSI information for its own cell with the other BSs via the backbone.

## 4.1 The System Model

We consider the downlink of a multicellular multiple input single output (MISO) OFDM network. There are a total of $M = 3$ cochannel users which are served by 3 base stations simultaneously. We assume that the resource allocation or scheduling has already been carried out and one user per cell is scheduled for transmission. For simplicity we assume that the BSs and the MSs are equipped with single antennas. Since the BSs cooperate with each other they act as a virtual MISO link. Since each user is equipped with a single antenna, to obtain diversity gain the cooperating BSs act as elements of a multiantenna system and utilize the Alamouti code to achieve transmit diversity. As pointed out in Chapter 3, transmit diversity is a crucial element for achieving high performance. Therefore we incorporate the Alamouti code and beamforming to the multicellular multiuser system. Several works have also considered using ST coding with beamforming [47, 48] and showed that it is beneficial to implement ST coding with beamforming to provide diversity when CSI is available at the transmitter.

We consider a system with the number of users are equal to 3 and there are 3 BSs cooperating such that in total we have $M_T = 3$ transmit antennas. We utilize OFDM transmission to combat frequency selective fading. By the use of OFDM, the channel is converted into a set of flat fading channels. For simplicity we will analyze the system model for subcarrier $k$, since the derivations will be easily extendable to all subcarriers. At subcarrier $k$, the user $i$ will observe the equivalent channel $\mathbf{h}_i(k)$ of size $(1 \times M_T)$ from the 3 BSs. Recall that this equivalent channel is the FFT of the time-domain frequency selective channel which was given in (3.3). The transmission schemes we consider incorporate the Alamouti code to achieve diversity since diversity is the key to superior error performance. Let the Alamouti coded data intended for user $i$ on subcarrier $k$ be

$$\mathbf{S}_i(k) = \begin{bmatrix} s_{i1} & -s_{i2}^* \\ s_{i2} & s_{i1}^* \end{bmatrix}. \tag{4.1}$$

Before transmission, for a given subcarrier $k$, the Alamouti code matrix for each user is multiplied with a transmit beamformer matrix, $\mathbf{W}_i(k)$ of size $(M_T \times 2)$, where $M_T = 3$ since we have 3 cooperating BSs. Each row of $\mathbf{W}_i(k)$ is chosen individually by a single BS and the 3 BSs cooperate for the transmission of every users' data. The overall data to be sent over the channel is the sum of all the

data intended for the $M = 3$ users, i.e.,

$$\mathbf{D}(k) = \sum_{m=1}^{M} \mathbf{W}_m(k)\mathbf{S}_m(k). \tag{4.2}$$

After OFDM demodulation, the received signal $\mathbf{y}_i(k)$ at subcarrier $k$ for user $i$ during two consecutive time durations is given by the $(1 \times 2)$ vector

$$\mathbf{y}_i(k) = \mathbf{h}_i(k)\mathbf{D}(k) + \mathbf{v}_i, \tag{4.3}$$

$$= \mathbf{h}_i(k)\mathbf{W}_i(k)\mathbf{S}_i(k) + \underbrace{\mathbf{h}_i(k) \sum_{\substack{m=1 \\ m \neq i}}^{M} \mathbf{W}_m(k)\mathbf{S}_m(k)}_{CCI} + \mathbf{v}_i, \tag{4.4}$$

where $\mathbf{v}_i$ is the noise vector which has i.i.d circularly symmetric complex Gaussian elements with variance $N_0$. The power normalization term $1/\sqrt{M_T}$ has been left out of equation (4.4) for simplicity.

In equation (4.4) the first term is the data for user $i$ while the second term is the CC caused by the other users' data. Our aim is to mitigate this CC term by appropriately choosing the beamformer matrices. We will consider a few methods to combat CC next.

### 4.1.1 Zero-Forcing Methods

Here we will consider is the zero-forcing (ZF) methods presented in [30-32] and [49]. In the ZF method the aim is to chose the beamformer matrices such that the CC term in (4.4) is equal to zero such that users cause no interference to each other. This can be expressed as

$$\mathbf{h}_i(k)\mathbf{W}_m(k) = \mathbf{0}, \quad \forall\ i, m = 1, ..., M, \quad i \neq m. \tag{4.5}$$

under the constraint that

$$\mathbf{W}_m^H \mathbf{W}_m = \mathbf{I}, \tag{4.6}$$

which ensures a constant transmission power for user $m$.

For notational brevity let us drop the subcarrier index $k$ in which case we mean that the operations presented below will be carried out for each subcarrier

index. Let $\hat{\mathbf{H}} = [\mathbf{h}_1^T \ \mathbf{h}_2^T \ \mathbf{h}_3^T]^T$ be all the collection of all the channels from all the BSs to every user, for a given subcarrier. For zero forcing at user $i$, we are interested in all of the channels except $\mathbf{h}_i$. Therefore we define the $(M-1) \times M_T$ matrix $\bar{\mathbf{H}}_i$ as

$$\bar{\mathbf{H}}_i = \left[\mathbf{h}_1^T \ ...\mathbf{h}_{i-1}^T \ \mathbf{h}_{i+1}^T ...\mathbf{h}_M^T\right]^T. \tag{4.7}$$

We want to find $\mathbf{W}_i$ such that

$$\bar{\mathbf{H}}_i \mathbf{W}_i = \mathbf{0}_{(2\times 2)}, \tag{4.8}$$

which establishes that other users data will not cause interference on user $i$. We may then compute the singular value decomposition (SVD) of $\bar{\mathbf{H}}_i$ as

$$\bar{\mathbf{H}}_i = \bar{\mathbf{U}}_i \bar{\mathbf{\Sigma}}_i \left[\bar{\mathbf{V}}_i^{(1)} \ \bar{\mathbf{V}}_i^{(0)}\right]^H, \tag{4.9}$$

where $\bar{\mathbf{V}}_i^{(0)}$ forms an orthogonal basis for the null space of $\bar{\mathbf{H}}_i$ and therefore it is the candidate for the columns of the beamforming matrix $\mathbf{W}_i$. In fact, with 3 users with single receive antennas and $M_T = 3$, there is only one column in the null space, therefore we duplicate this column to form $\mathbf{W}_i$. This means that both columns of $\mathbf{W}_i$ are the same.

### 4.1.2 Signal to Leakage Ratio Method

In this scheme the authors define a new metric called leakage and try to minimize the leakage while designing the transmit beamforming matrices [37]. CC is the interference created by the other users on the desired users signal, whereas leakage is the interference caused by the signal intended for a desired user on the remaining users. Leakage is a measure of how much signal power leaks into other users. Instead of maximizing SINR, the authors provide a technique which will maximize signal to leakage ratio (SLNR). The advantage of this scheme is that while the SINR maximization problem is very complicated, SLNR maximization criterion has a closed form solution.

The SINR ratio may be computed from (4.4) as [37]

$$\mathrm{SINR_i(k)}=\frac{\|\mathbf{H}_\mathrm{i}(\mathrm{k})\mathbf{W}_\mathrm{i}(\mathrm{k})\|_\mathrm{F}^2}{\sum\limits_{\mathrm{m=1,m\neq i}}^{\mathrm{M}}\|\mathbf{H}_i(\mathrm{k})\mathbf{W}_m(\mathrm{k})\|_\mathrm{F}^2+\mathrm{N}_0}. \tag{4.10}$$

It can be seen that maximizing SINR for each user $i$ involves the knowledge of other users beamforming matrices, $\mathbf{W}_m(\mathrm{k})$ for all $m \neq i$. Therefore this is a complicated problem with $M$ coupled matrices $\mathbf{W}_m(\mathrm{k})$ for all $m = 1, ..., M$.

The SLNR for user $i$ may be expressed as

$$\mathrm{SLNR_i(k)} = \frac{\|\mathbf{H}_\mathrm{i}(\mathrm{k})\mathbf{W}_\mathrm{i}(\mathrm{k})\|_\mathrm{F}^2}{\sum\limits_{\mathrm{m=1,m\neq i}}^{\mathrm{M}}\|\mathbf{H}_\mathrm{m}(\mathrm{k})\mathbf{W}_\mathrm{i}(\mathrm{k})\|_\mathrm{F}^2+\mathrm{N}_0}. \tag{4.11}$$

It can be seen that the SLNR for user $i$ depends only on the beamformer matrix associated with that user, i.e., $\mathbf{W}_i(k)$. Therefore the beamformer matrix may be computed for each user independently of other users' beamformer matrices. It was shown in [37] that each column of $\mathbf{W}_i(k)$ may be chosen according to

$$\text{max. eigenvector}\left(\left(N_0\mathbf{I}+\bar{\mathbf{H}}_i(k)^H\bar{\mathbf{H}}_i(k)\right)^{-1}\mathbf{H}_i(k)^H\mathbf{H}_i(k)\right), \tag{4.12}$$

where max. eigenvector($\mathbf{x}$) denotes the eigenvector corresponding to the largest eigenvalue of $\mathbf{x}$.

## 4.2 Randomized Space-Time Coding

Randomized space-time coding was proposed in [50] to the problem where a group of $P$ nodes are trying to communicate the same message to a single receiver. The transmitters and receiver have only a single antenna, however by to the proper usage of a randomization matrix the transmitting nodes make use of the distributed Alamouti coding scheme for transmission. For this, the source symbols are first mapped to the Alamouti space-time code (STC) matrix $\mathbf{C}$

previously shown in (2.18). Since each transmitter has only one transmit antenna, at each time slot the transmitter sends a linear combination of the columns of the Alamouti matrix. The linear combination is obtained by the use of the randomization matrix, where each transmitter picks a random row to multiply with the Alamouti STC matrix. For simplicity the channel is assumed to be flat fading. The received signal can be expressed as

$$\mathbf{y} = \mathbf{hRC} + \mathbf{n}, \tag{4.13}$$

where the $P\times$ 2 randomization matrix is $\mathbf{R} = \begin{bmatrix}\mathbf{r}_1^T & \mathbf{r}_2^T & ... & \mathbf{r}_N^T\end{bmatrix}^T$. Each node $i$ will chose the randomization vector $\mathbf{r}_i$ to multiply with the STC matrix. This way each node may chose from a given distribution the $\mathbf{r}_i$'s independently from each other which allows for a decentralized transmission scheme. The end receiver decodes the signal by estimating the equivalent channel $\tilde{\mathbf{h}} = \mathbf{hR}$.

We consider two choices for the matrix $\mathbf{R}$. The first one is where the rows of $\mathbf{R}$ are chosen from a spherical Gaussian distribution, i.e., $\mathbf{r}_i$'s are chosen as zero-mean independent complex Gaussian vectors with covariance $\mathbf{I}$ and are normalized to have norm equal to 1. The second one is the centralized scheme where half of the nodes are chosen to serve as the first antenna and the second half are chosen to serve as the second antenna. When $P$ is odd, at one of the nodes the power is distributed equally between two antennas, i.e., for $P = 3$

$$R = \begin{bmatrix} 1 & 0 \\ 0 & 1 \\ 1/\sqrt{2} & 1/\sqrt{2} \end{bmatrix}. \tag{4.14}$$

Our aim is to adapt this method to the BS cooperation for CC mitigation problem. The $P$ nodes now become the BSs cooperating to send data to a user. In [50] it was shown that the best performance is achieved when the centralized scheme is used. Since BSs are connected to each other we can relax the distributedness constraint and focus on this centralized case. For the centralized case we begin by computing the covariance matrix of the equivalent channel matrix from the 3 BSs to user $i$ by $\tilde{\mathbf{h}}_i = \mathbf{h}_i\mathbf{R}$, which is given by

$$\mathrm{Cov}(\tilde{\mathbf{h}}_\mathrm{i}) = \mathrm{E}\big[\,(\mathbf{h}_\mathrm{i}\mathbf{R})^\mathrm{H}\,(\mathbf{h}_\mathrm{i}\mathbf{R})\,\big]. \tag{4.15}$$

The covariance matrix of $\tilde{\mathbf{h}}_i$ may be computed as follows. We can express $\mathbf{h}_i$ as the small-scale fading coefficient from $\alpha_{ij}$ BS $j$ to user $i$ divided by the square

root of the path loss $Pl_{ij}$ coefficient.

$$\mathbf{h}_i = \left[ \begin{array}{ccc} \frac{\alpha_{i1}}{\sqrt{Pl_{i1}}} & \frac{\alpha_{i2}}{\sqrt{Pl_{i2}}} & \frac{\alpha_{i3}}{\sqrt{Pl_{i3}}} \end{array} \right]. \tag{4.16}$$

Recall that path loss is related to the distance between the user $i$ and the BS $j$ as $Pl_{ij} = d_{ij}^n$ where $n$ is the path loss exponent. $\tilde{\mathbf{h}}_i = \mathbf{h}_i\mathbf{R}$ may be computed using (4.16) as

$$\mathbf{h}_i\mathbf{R} = \left[ \begin{array}{ccc} \frac{\alpha_{i1}}{\sqrt{Pl_{i1}}} & \frac{\alpha_{i2}}{\sqrt{Pl_{i2}}} & \frac{\alpha_{i3}}{\sqrt{Pl_{i3}}} \end{array} \right] \left[ \begin{array}{cc} 1 & 0 \\ 0 & 1 \\ 1/\sqrt{2} & 1/\sqrt{2} \end{array} \right], \tag{4.17}$$

$$= \left[ \begin{array}{cc} \frac{\alpha_{i1}}{\sqrt{Pl_{i1}}} + \frac{\alpha_{i3}}{\sqrt{2Pl_{i3}}} & \frac{\alpha_{i2}}{\sqrt{Pl_{i2}}} + \frac{\alpha_{i3}}{\sqrt{2Pl_{i3}}} \end{array} \right]. \tag{4.18}$$

By using this we may compute the following expectation

$$E\left[\tilde{\mathbf{h}}_i^H \tilde{\mathbf{h}}_i\right] = E\left[ \left[ \begin{array}{c} \frac{\alpha_{i1}^*}{\sqrt{Pl_{i1}}} + \frac{\alpha_{i3}^*}{\sqrt{2Pl_{i3}}} \\ \frac{\alpha_{i2}^*}{\sqrt{Pl_{i2}}} + \frac{\alpha_{i3}^*}{\sqrt{2Pl_{i3}}} \end{array} \right] \left[ \begin{array}{cc} \frac{\alpha_{i1}}{\sqrt{Pl_{i1}}} + \frac{\alpha_{i3}}{\sqrt{2Pl_{i3}}} & \frac{\alpha_{i2}}{\sqrt{Pl_{i2}}} + \frac{\alpha_{i3}}{\sqrt{2Pl_{i3}}} \end{array} \right] \right], \tag{4.19}$$

and by noting that $\alpha_{ij}$'s are i.i.d Gaussian random variables with unit variance, the above expectation is equal to

$$\mathrm{Cov}(\tilde{\mathbf{h}}_\mathrm{i}) = \mathrm{E}\big[ \left(\mathbf{h}_\mathrm{i}\mathbf{R}\right)^\mathrm{H} \left(\mathbf{h}_\mathrm{i}\mathbf{R}\right) \big] = \left[ \begin{array}{cc} \frac{1}{Pl_{i1}} + \frac{1}{2Pl_{i3}} & \frac{1}{2Pl_{i3}} \\ \frac{1}{2Pl_{i3}} & \frac{1}{Pl_{i2}} + \frac{1}{2Pl_{i3}} \end{array} \right]. \tag{4.20}$$

We may now choose the transmit beamforming matrices such that the CC is completely canceled and non-zero part of the product of the channel matrix and beamformer matrix has elements with covariance given in (4.20). This way we are able to achieve the performance of the centralized scheme by BS cooperation with no CC degradation. Again for simplicity we drop the subcarrier index $k$ and note that the below operations will be carried out at each subcarrier index. For example, $\mathbf{W}_1$ may be computed from

$$\hat{\mathbf{H}}\mathbf{W}_1 = \left[ \begin{array}{cc} a & b \\ 0 & 0 \\ 0 & 0 \end{array} \right], \tag{4.21}$$

where the variables (a,b) are computed according to

$$[a\ b] = \left(\mathrm{Cov}(\tilde{\mathbf{h}}_i)^{1/2}\mathbf{x}\right)^T. \tag{4.22}$$

We use this method because while completely canceling out CC we wish to have error performance similar to the centralized case presented above. By the use of the covariance matrix, we can mimic the equivalent channel that would have existed if there were only a single user being served by the BSs which were using the centralized transmission scheme parameters.

In (4.22), the $(2 \times 1)$ the random vector $\mathbf{x}$ has complex Gaussian elements with unit variance. Similarly to (4.21) $\mathbf{W}_2$ and $\mathbf{W}_3$ are computed from

$$\hat{\mathbf{H}}\mathbf{W}_2 = \begin{bmatrix} 0 & 0 \\ a & b \\ 0 & 0 \end{bmatrix}, \quad \hat{\mathbf{H}}\mathbf{W}_3 = \begin{bmatrix} 0 & 0 \\ 0 & 0 \\ a & b \end{bmatrix}, \tag{4.23}$$

with different realizations for each (a,b) pair.

## 4.3 Simulation Results

We consider a hexagonal cellular structure with radius equal to 1 km. Each cell is separated into three 120 degree sectors by the BSs which use directional antennas. The area of interest is the intersection of 3 neighboring cells and CC is assumed to be limited to this area where BSs can make transmissions as a collaborative MISO system. We assume that a user in each cell has been scheduled such that there are 3 users receiving data from the 3 BSs simultaneously. Each user considers the nearest BS as its own BS.

The performance of various techniques are investigated for 100 random location scenarios for each user, where users are uniformly distributed in the area of interest at least 100 meters away from their BSs, with the constraint that there are equal number users in each sector. Figure 4.1 depicts the user locations in each cell. To obtain reliable results, for each user we will evaluate the error performance of each technique for these 100 different locations and average the results.

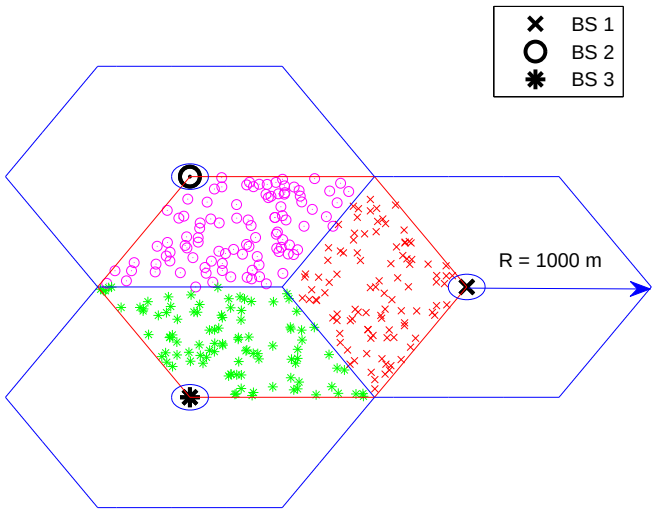


Figure 4.1: User locations.

We also incorporate large scale fading which was ignored in Chapter 3. Since we are considering the performance in a multicellular environment, path loss becomes an important factor. We choose the path loss exponent equal to $n = 3.76$. We use the ITU Ped-B channel model with user mobility $v = 3$ km/hr. The subchannelization scheme is Band AMC. For simplicity the modulation scheme is chosen as BPSK. The OFDM parameters are chosen as those given in Table 3.1. All users share all the available subcarriers. Moreover, FEC is not implemented.

We do not use per BS power constraints but instead use total power constraints where the BSs share the available power. To this end, the following normalization is carried out

$$\left(\mathbf{W}_m(\mathrm{k})\right)^H \mathbf{W}_m(\mathrm{k}) = \mathbf{I}, \quad m = 1, ..., M. \tag{4.24}$$

To combat path loss all the BSs multiply their data with a factor of $\sqrt{\frac{P}{M_T}}$ where $P$ is chosen as $P = 1000^n$ so that the user the farthest (1000 m) away from its BS will receive signals which have at least the transmitted power. Of course by doing this users closer to the BSs will receive higher signal power.

We evaluate the performance of 4 transmission techniques.

1. The first technique we consider is the no interference case. In this scheme the BSs transmit to a single user in one of the cells. This way there is no CC caused by data intended for other users. The performance of this scheme is investigated as a benchmark and to serve as a lower bound on performance. For this scheme we consider the decentralized spherical and the centralized distributed STC. We will refer to these schemes as Spherical-No Coop and Centralized-No Coop, respectively. We use the phrase "No Coop" because although 3 BSs are cooperating to serve a single user there is no system-wide cooperation, i.e., 3 BSs serving 3 users simultaneously.

2. The second scheme is the ZF scheme described in Section 4.1.1. We will refer to this scheme as ZF using SVD.

3. The third scheme is the SLNR scheme described in Section 4.1.2.

4. The final scheme is the randomized space-time coded BS cooperation scheme described in Section 4.2 in equations (4.21)-(4.23). We will refer to this scheme as ZF using Covariance.

It should be noted that CSI for all users is assumed to be present at all of the BSs.

We begin by evaluating the effects of CC on the performance of each user if CC is not mitigated. We assume that the CC given in (4.4) is treated as additional noise at the receiver. We compare the performance of the system when 3 BSs are serving a single user only, i.e., there is no CC, and the case where all the users are being served simultaneously by the 3 BSs such that there is significant CC. It can be seen in Figures 4.2-4.4 that when CC is not mitigated it is detrimental to system performance. The performance is plotted against average received power. The average received power for each user is different due to the difference in locations.

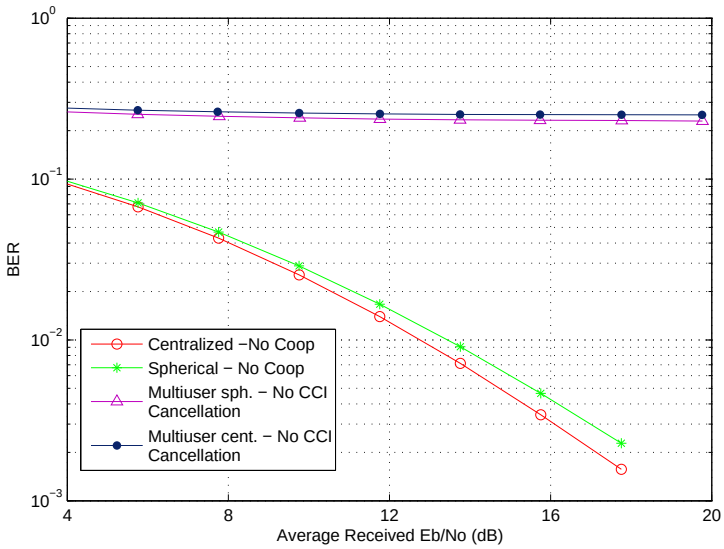


Figure 4.2: User 1 performance with and without CC.

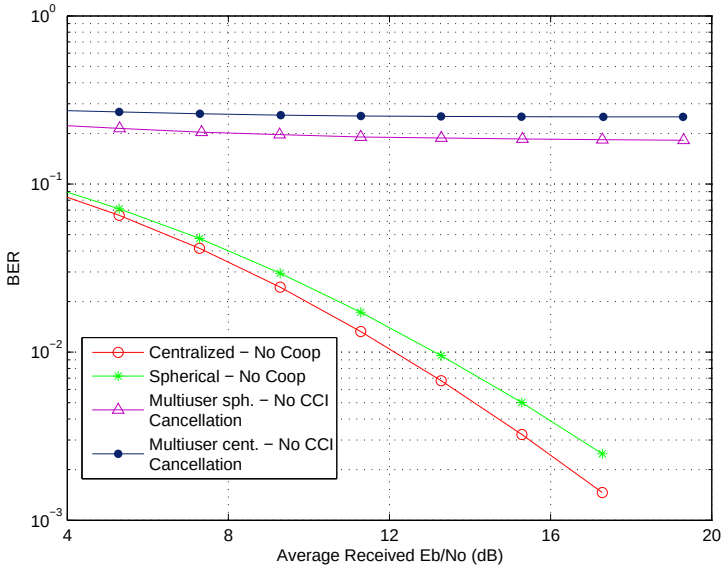


Figure 4.3: User 2 performance with and without CC.

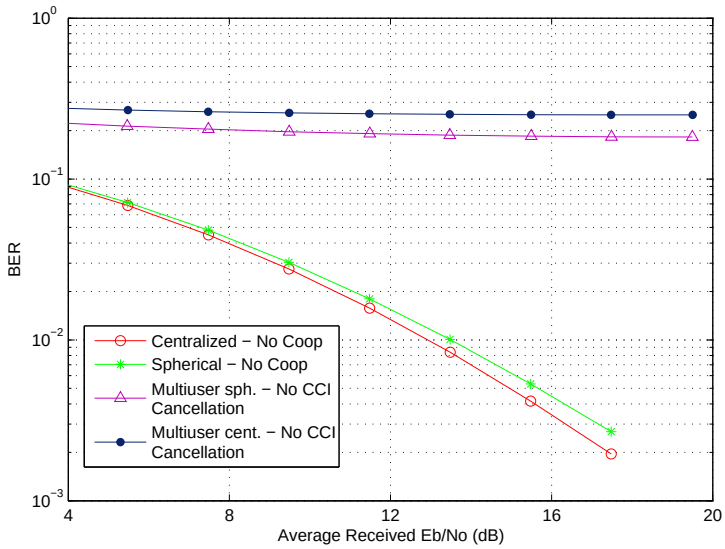


Figure 4.4: User 3 performance with and without CC.

We present the performance of the 4 transmission schemes mentioned earlier for each user in Figures 4.5-4.7. Again we plot the performance against average received power.

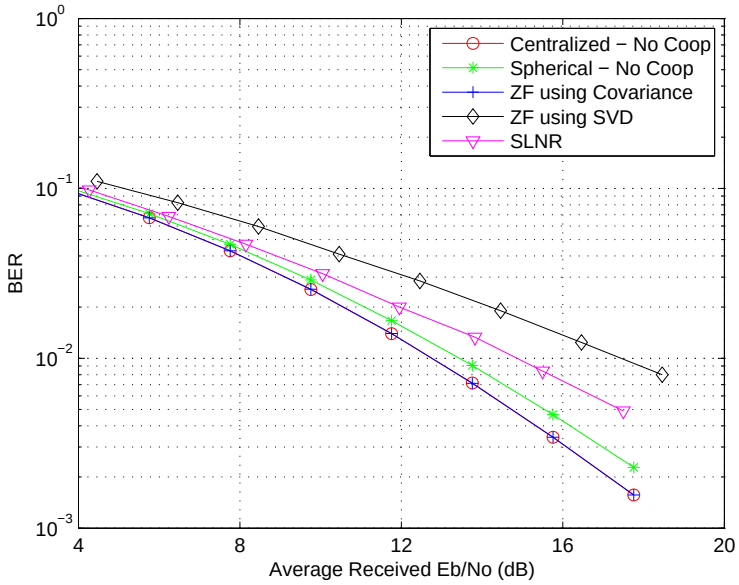


Figure 4.5: User 1 performance under various transmission schemes.

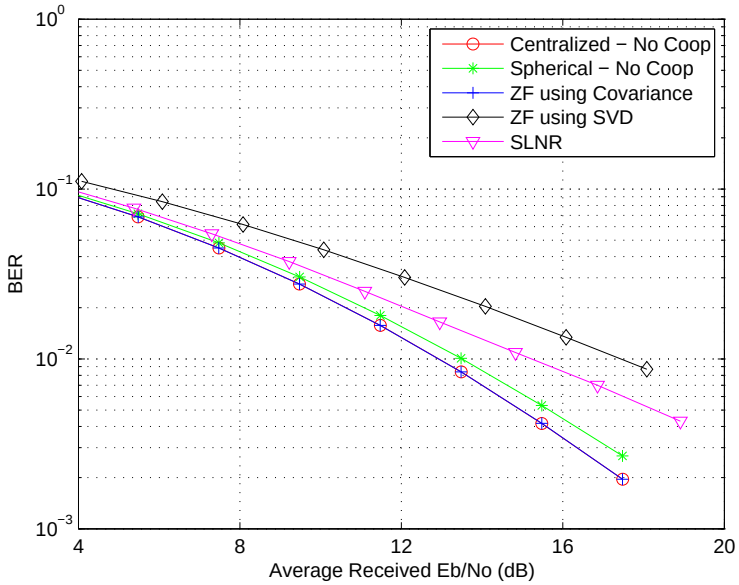


Figure 4.7: User 3 performance under various transmission schemes.

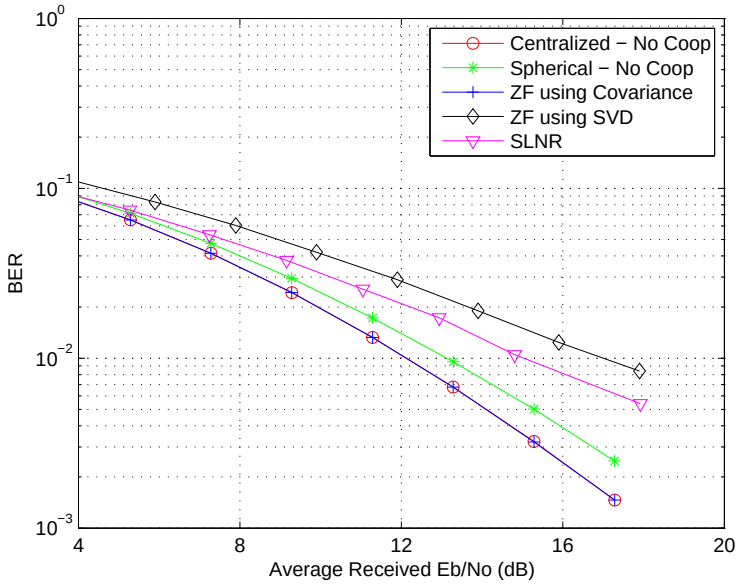


Figure 4.6: User 2 performance under various transmission schemes.

It can be seen that the ZF method using SVD has the worst performance followed by SLNR. The performance of ZF using covariance is the same as the no interference case which shows that CC is successfully eliminated. This way 3 users may share the same bandwidth without any loss in performance.

The main drawback of the schemes we have considered is that full CSI knowledge is needed at the BSs to determine the beamforming matrix $\mathbf{W}_i$. This is especially cumbersome for OFDM since the channel gains at each subcarrier must be shared among the BSs which may require additional bandwidth to be allocated for sharing purposes.

# Chapter 5

# Conclusions

In this thesis we have considered two different aspects of MIMO-OFDM communication systems. Firstly, we have evaluated the performance of different FEC and MIMO techniques on the error performance of a single link when only a single user is being served by a BS and with only small-scale fading effects taken into account. Secondly, we consider a multicellular system where BSs cooperate with each other to simultaneously serve 3 users who are in different cells. We analyze the performance of different cooperative transmission schemes.

In the first part of the thesis we have described MIMO-OFDM systems and given an introduction to the IEEE 802.16 (WiMAX) standard. Our main focus was on the PHY layer. Afterwards we have evaluated the performance of the WiMAX PHY layer through simulations.

Firstly the performance of the system without FEC was investigated. It was shown that when there is mobility in the channel, the channel variations have a negative effect on ST-Alamouti performance. This is because the assumption that the channel stays constant for 2 OFDM symbol durations is no longer valid and to maintain linear decoding complexity, the decisions made with constant channel assumption lead to performance losses. Specifically, an error floor is clearly observed especially at $v = 120$ km/hr. To combat this irreducible error floor at high mobilities, we may choose SF-Alamouti.

Although SF-Alamouti is advantageous in the case of mobility, it too suffers from a drawback. It was stated that SF-Alamouti relies on adjacent subcarriers to be identical for optimal linear decoding, but there may be variations between the subcarriers due to the frequency selective nature of the channel. However

since the FFT size we consider is larger, these variations are minimal and each subcarrier pair may be assumed identical in the decoding process which remains linear with this assumption. Therefore we may state that the variation of the channel response between adjacent symbol intervals caused by mobility is much more severe than the variation between subcarriers caused by high delay spread. Therefore, it is more feasible to use SF-Alamouti than ST-Alamouti.

When a rate of 2 symbols/pcu is desired, SM or the Golden Code may be employed. SM has worse performance when compared to ST-Alamouti. This is because SM does not make use of transmit diversity which is crucial for superior error performance. However even though the Golden Code incorporates transmit diversity, it also suffers from mobility since its decoding process also relied on constant channel assumption of two consecutive OFDM symbols.

Secondly, after FEC was added to the system, coding gain was observed. We have considered CC and CTC both with rates 1/2. It was shown that increasing the FEC block size from 96 bits to 480 bits has improved the performance. It was also shown that CTC outperforms CC. We have considered only a few of the modulation and coding scenarios present in the standard, but it is clear that the choice of modulation and coding plays an important role in error performance.

We have also proposed a SF code based on the TAST framework. This code originally had a decoding complexity of $|\mathcal{M}|^8$, which is extremely prohibitive. However by making use of the algorithm presented in [9], we were able to reduce the decoding complexity to $|\mathcal{M}|^4$. It was shown that the TAST code has a superior performance and a rate of 2 symbols/pcu, but to be of practical value we must reduce the decoding complexity further.

We have also analyzed the performance of different subchannelization schemes, band AMC and PUSC. Band AMC uses contiguous subcarriers to form subchannels whereas PUSC uses pseudorandomly distributed subcarriers to form subchannels. The assumption of identical channel gains for every pair of subcarriers in the case of SF-Alamouti were true when band AMC is used. However when PUSC is used, the data symbols are mapped to random subcarriers which are usually far away enough from each other such that the variation between these subcarriers no longer has negligible effect on performance. Therefore when SF codes are used in conjunction with PUSC there is a severe performance degradation. However in the case of ST code, PUSC provides some additional frequency diversity which results in improved performance.

Another important issue in OFDM communications is ICI which arises as a result of time variation present in the channel or frequency synchronization errors. We have assumed perfect frequency synchronization and only analyzed the case when ICI is caused by mobility. An analysis of ICI was given and some simulations regarding the effects of ICI on the performance were presented. It was shown that ICI has a negative effect on performance which becomes more severe at higher SNRs.

As future work, TAST codes with acceptable decoding complexity will be investigated since they achieve good performance at high data rates. Moreover, in this thesis we have considered only a few of the modulation and coding scenarios present in the IEEE 802.16 standard. As a future work, we may simulate the performance of the other profiles stated in IEEE 802.16 standard to generate look-up tables which are useful for PHY abstractions considered when simulating the performance of higher layers.

In the second part of the thesis we have evaluated the performance of cooperative data transmission schemes. We assumed that scheduling has already been done and we are interested in the performance of various cooperative transmission schemes. We consider the scenario where 3 BSs cooperate to serve 3 users simultaneously while using the same frequency band, i.e., with a frequency reuse factor of 1. When a frequency factor of 1 is used there is high spectral efficiency in the system however the performance is severely limited by CC. BS cooperation offers a promising solution to mitigate CC in multicellular networks with a frequency reuse factor of 1.

The MSs are desired to be as simple as possible therefore CC mitigation is carried out by the BSs. To mitigate CC we consider ZF schemes since they are simple to implement and also consider the SLNR scheme which tries to minimize the leakage a users data may cause on other users. We propose a different ZF method which relies on the covariance matrix of the transmit beamforming matrix when no CC is present, i.e., all BSs are serving a single user. This way we are able to approach the error performance of the system where BSs are serving a single user, when actually the CC is mitigated and all BSs are cooperating to serve 3 users simultaneously. We have also incorporated the Alamouti scheme which results in superior error performance with low decoding complexity, as was shown in the first part of the thesis.

However, in all of the mentioned schemes we have assumed full CSI at the BSs. This CSI may be obtained in the uplink stage and each BS may share

the CSI of the user in its own cell with other cooperating BSs. Furthermore, it may be possible to share this information less frequently if the channel is slowly varying, i.e., user mobility is low.

As future work we must investigate the practical issues concerning BS cooperation and make it more implementable in practical systems. The first step must be to find an algorithm which does not require exact CSI at the BSs to form the transmit beamforming matrices. Secondly, it is desirable to make the algorithm decentralized such that each BS may decide on the transmit beamformer on its own without sharing any data with other BSs.

Another important issue concerning our algorithm may be how accurately the distances between BSs and users are determined. This may be an important problem if the users have high mobility. Furthermore, synchronization is also very important for cooperative systems. It was assumed that there exists perfect frequency and timing synchronization between the BSs and there may be performance losses due to synchronization errors.

# Bibliography


[1] T. S. Rappaport, *Wireless Communicatios:Principles and Practice, 2nd ed.* Prentice Hall, 2002.

[2] E. Telatar, "Capacity of multi-antenna gaussian channels," *European Transactions on Telecommunications*, vol. 10, no. 6, pp. 585–596, Nov. 1999.

[3] G. J.Foschini and M. J. Gans, "On limits of wireless communications in a fading environment when using multiple antennas," *Wireless Personal Communications*, vol. 6, no. 3, pp. 311–335, Mar. 1998.

[4] G. J.Foschini, "Layered space-time architecture for wireless communication in a fading environment when using multiple-element antennas," *Bell Labs Technical Journal*, vol. 1, no. 2, pp. 41–59, Aug. 1996.

[5] A. F. Naguib, N. Seshadri, and A. R. Calderbank, "Increasing data rate over wireless channels," *IEEE Signal Processing Magazine*, vol. 17, no. 3, pp. 76–92, May 2000.

[6] V. Tarokh, N. Seshadri, and A. R. Calderbank, "Space-time codes for high data rate wireless communication: performance criterion and code construction," *IEEE Transactions on Information Theory*, vol. 44, no. 2, pp. 744–765, Mar. 1998.

[7] S. M. Alamouti, "A simple transmit diversity technique for wireless communications," *IEEE Journal on Selected Areas in Communications*, vol. 16, no. 8, pp. 1451–1458, Oct. 1998.

[8] V. Tarokh, H. Jafarkhani, and A. Calderbank, "Space-time block codes from orthogonal designs," *IEEE Transactions on Information Theory*, vol. 45, no. 5, pp. 1456–1467, Jul. 1999.

[9] S. Sezginer and H. Sari, "Full-rate full-diversity 2x2 space-time codes of reduced decoder complexity," *IEEE Communications Letters*, vol. 11, no. 12, pp. 973–975, Dec. 2007.

[10] J. C. Belfiore, G. Rekaya, and E. Viterbo, "The golden code: a 2x2 full-rate space-time code with non-vanishing determinants," *IEEE Transactions on Information Theory*, vol. 51, no. 4, pp. 1432–1436, Apr. 2005.

[11] H. E. Gamal and M. O. Damen, "Universal space-time coding," *IEEE Transactions on Information Theory*, vol. 49, no. 5, pp. 1097–1119, May 2003.

[12] M. O. Damen, K. Abed-Meraim, and J. C. Belfiore, "Diagonal algebraic space-time block codes," *IEEE Transactions on Information Theory*, vol. 48, no. 3, pp. 628–636, Mar. 2002.

[13] X. Giraud, E. Boutillon, and J. C. Belfiore, "Algebraic tools to build modulation schemes for fading channels," *IEEE Transactions on Information Theory*, vol. 43, no. 3, pp. 938–952, May 1997.

[14] D. Tse and P. Viswanath, *Fundamentals of Wireless Communication.* Cambridge Univ. Press, 2005.

[15] D. Agrawal, V. Tarokh, A. Naguib, and N. Seshadri, "Space-time coded OFDM for high data-rate wireless communication over wideband channels," in *Proc. IEEE Vehicular Technology Conference*, Ottawa, Canada, May 1998, pp. 2232 – 2236.

[16] K. Lee and D. Williams, "A space-frequency transmitter diversity technique for OFDM systems," in *Proc. IEEE GLOBECOM*, San Francisco, USA, Nov. 2000, pp. 1473–1477.

[17] B. Lu and X. Wang, "Space-time code design in OFDM systems," in *Proc. IEEE GLOBECOM*, San Francisco, USA, Nov. 2000, pp. 1000–1004.

[18] H. Bölcskei and A. J. Paulraj, "Space-frequency coded broadband OFDM systems," in *Proc. IEEE Wireless Communications and Networking Conference*, Chicago, USA, Sep. 2000, pp. 1–6.

[19] W. Su, Z. Safar, M. Olfat, and K. J. R. Liu, "Obtaining full-diversity space-frequency codes from space-time codes via mapping," *IEEE Trans. Signal Proc.*, vol. 51, no. 11, pp. 2905–2916, Nov. 2003.

[20] B. Lu and X. Wang, "Space-time code design in OFDM systems," in *Proc. IEEE GLOBECOM*, San Francisco, USA, Nov. 2000, pp. 1000–1004.

[21] H. Bölcskei and A. J. Paulraj, "Space-frequency codes for broadband fading channels," in *Proc. IEEE Int. Symp. Information Theory*, Washington DC, USA, Jun. 2000, p. 219.

[22] W. Su, Z. Safar, and K. J. R. Liu, "Full-rate full-diversity space-frequency codes with optimum coding advantage," *IEEE Transactions on Information Theory*, vol. 51, no. 1, pp. 229–249, Jan. 2005.

[23] J. Boutros and E. Viterbo, "Signal space diversity: A power and bandwidth efficient diversity technique for the Rayleigh fading channel,," *IEEE Transactions on Information Theory*, vol. 44, no. 4, pp. 1453–1467, Jul. 1998.

[24] W. Zhang, X. G. Xia, and P. C. Ching, "High-rate full-diversity space-time-frequency codes for broadband MIMO block-fading channels," *IEEE Trans. Communications*, vol. 55, no. 1, pp. 25–34, Jan. 2007.

[25] Z. Liu, Y. Xin, and G. Giannakis, "Space-time-frequency coded OFDM over frequency selective fading channels," *IEEE Transactions on Signal Processing*, vol. 50, no. 10, pp. 2465–2476, Oct. 2002.

[26] K. Karakayali, G. J. Foschini, R. A. Valenzuela, and R. D. Yates, "On the maximum common rate achievable in a coordinated network," in *Proc. IEEE International Conference on Communications*, Istanbul, Turkey, Jun. 2006, pp. 4333–4338.

[27] M. Costa, "Writing on dirty paper," *IEEE Transactions on Information Theory*, vol. 29, no. 3, pp. 439–441, May 1983.

[28] G. Caire and S. Shamai(Shitz), "On the achievable throughput of a multi-antenna gaussain broadcast channel," *IEEE Transactions on Information Theory*, vol. 49, no. 9, pp. 1691–1706, Jul. 2003.

[29] T. Yoo and A. Goldsmith, "Optimality of zero-forcing beam forming with multiuser diversity," in *Proc. IEEE International Conference on Communications*, Seoul, Korea, May 2005, pp. 542–546.

[30] H. Zhang, H. Dai, and Q. Zhou, "Base station cooperation for multiuser MIMO: Joint transmission and BS selection," in *Proc. Conference on Information Sciences and Systems*, Princeton University Princeton, USA, Mar. 2004.

[31] Q. H. Spencer, A. L. Swindlehurst, and M. Haardt, "Zero-forcing methods for downlink spatial multiplexing in multi-user MIMO channels," *IEEE Transactions on Signal Processing*, vol. 52, no. 2, pp. 461–471, Feb. 2004.

[32] J. G. A. R. Chen and R. W. Heath, "Multiuser space-time block coded MIMO system with downlink preceding," in *Proc. IEEE Int. Conf. Commun.*, Paris, France, Jun. 2004, pp. 2689–2693.

[33] Z. Pan, K.-K. Wong, and T.-S. Ng, "Generalized multiuser orthogonal space-division multiplexing," *IEEE Transactions on Wireless Communications*, vol. 3, no. 6, pp. 1969–1973, Nov. 2004.

[34] M. Schubert and H. Boche, "Solution of the multiuser downlink beamforming problem with individual SINR constraints," *IEEE Transactions on Vehicular Technology*, vol. 53, no. 1, pp. 18–28, Jan. 2004.

[35] F. R. Farrokhi, K. J. R. Liu, and L. Tassiulas, "Transmit beamforming and power control for cellular wireless systems," *IEEE Select. Areas Commun.*, vol. 16, no. 8, pp. 1437–1450, Oct. 1998.

[36] P. Viswanath and D. Tse, "Sum capacity of the vector gaussian broadcast channel and uplink-downlink duality," *IEEE Transactions on Information Theory*, vol. 49, no. 8, pp. 1912– 1921, Aug. 2003.

[37] M. Siddek, A. Tarighat, and A. H. Sayed, "A leakage-based precoding scheme for downlink multi-user MIMO channels," *IEEE Transactions on Wireless Communications*, vol. 6, no. 5, 2007.

[38] A. Goldsmith, *Wireless Communications*. Cambridge University Press, 2005.

[39] B. Vucetic and J. Yuan, *Space-Time Coding*. John Wiley & Sons, 2003.

[40] R. A. Horn and C. R. Johnson, *Matrix Analysis*. Cambridge Univ. Press, 1988.

[41] *Local and Metropolitan Area Networks Part 16: Air Interface for Fixed and Mobile Broadband Wireless Access Systems*, IEEE P802.16Rev2/D7 October 2008 Std.

[42] *802.16m Evaluation Methodology Document*, IEEE 802.16m-2008 Std.

[43] D. T. Harvatin and R. E. Ziemer, "Orthogonal frequency division multiplexing performance in delay and doppler spread channels,," in *Proc. IEEE Vehicular Technology Conference*, Phoenix, AZ, USA,, May 1997, pp. 1644–1647.

[44] *Local and Metropolitan Area Networks Part 16: Air Interface for Fixed and Mobile Broadband Wireless Access Systems*, IEEE 802.16e-2005 Std.

[45] J. G. Andrews, A. Gnosh, and R. Muhamed, *Fundamentals of WiMAX: Understanding Broadband Wireless Networking*. Prentice Hall, 2007.

[46] A. Stamoulis, S. N. Diggavi, and N. Al-Dhahir, "Intercarrier interference in MIMO-OFDM," *IEEE Trans. Signal Process.*, vol. 50, no. 10, pp. 2451–2464, Oct. 2002.

[47] D. Z. Filho, L. Fety, and J. Romano, "Adding diversity to multi-user downlink beamforming by using ber constraints,," in *2006 International Telecommunications Symposium*, Fortaleza-Ce, Brazil, Sep. 2006, pp. 672–677.

[48] G. Jöngren, M. Skoglund, and B. Ottersten, "Combining beamforming and orthogonal space-time block coding," *IEEE Transactions on Information Theory*, vol. 48, no. 3, pp. 611–627, Mar. 2002.

[49] K. Karakayali, R. Yates, G. Foschini, and R. Valenzuela, "Optimum zero-forcing beamforming with per-antenna power constraints," in *Proc. IEEE Int. Symp. Information Theory*, Nice, France, Jun. 2007, pp. 101–105.

[50] B. Sirkeci-Mergen and A. Scaglione, "Randomized space-time coding for distributed cooperative communication," *IEEE Transactions on Signal Processing*, vol. 55, no. 10, pp. 5003–5017, Oct. 2007.